



CHALMERS

Pulse-Electroplating: Process Parameters and Their Influence on the Formed Microstructure

Diploma work in the Master Programme Materials Engineering

DANIEL MELCIU
NAVIN MAIDEE

Pulse-Electroplating: Process Parameters and Their Influence on the Formed Microstructure

by

Daniel Melciu
Navin Maidee

Diploma work No. 161/2015
at Department of Materials and Manufacturing Technology
CHALMERS UNIVERSITY OF TECHNOLOGY
Gothenburg, Sweden

Diploma work in the Master Programme Materials Engineering

Performed at: Department of Materials and Manufacturing Technology
Chalmers University of Technology
SE-41296 Gothenburg

Examiner & Supervisor: Professor Uta Klement
Department of Materials and Manufacturing Technology
Chalmers University of Technology
SE-41296 Gothenburg

Pulse-Electroplating: Process Parameters and Their Influence on the Formed Microstructure

Daniel Melciu
Navin Maidee

© Daniel Melciu, 2015

© Navin Maidee, 2015

Diploma work No. xx/2015
Department of Materials and Manufacturing Technology
Chalmers University of Technology
SE-412 96 Gothenburg
Sweden
Telephone + 46 (0)31-772 1000

Pulse-Electroplating: Process Parameters and Their Influence on the Formed Microstructure

Daniel Melciu
Navin Maidee

Department of Materials and Manufacturing Technology
Chalmers University of Technology

Abstract

Nickel-layers with a thickness of a few tens of microns were produced by pulse-electrodeposition using two electrolytic baths (I and II). The influence of temperature and current density on the obtained microstructure was investigated using Electrolyte I while for the effect of Nickel Sulfamate concentration and current density was analyzed using Electrolyte II. In addition, Polyamide fibers included in Hybrix™ sandwich material were coated by pulse-electrodeposition and afterwards investigated. Electrodeposited Nickel was examined in the as-prepared state by XRD and SEM. With the help of EBSD technique, orientation maps, pole figures and inverse pole figures were obtained for all samples. Different microstructures were obtained by changing temperature and current density. As a result, the average grain size of as-deposited Nickel varied from 30 nm to 200 nm, depending on plating conditions. Moreover, a <100>-texture is obtained independently of plating conditions. In contrast, when the effect of Nickel Sulfamate concentration and current density was investigated, no preferred orientation, i.e. a weak <110>-texture is attained independently on Nickel Sulfamate concentration and current density. The average grain size of the produced microstructures was in the range of 40 to 50 nm. Concerning the electrodeposition on Polyamide fibers, a Nickel coating was successfully deposited on the fibers.

Keywords: Nickel electrodeposition, pulse-electrodeposition, texture, microstructure, nanocrystalline structure, EBSD

Table of Contents

1 Introduction.....	1
1.1 Electrodeposition	1
1.2 Electrodeposited Nanocrystalline Structure	2
1.3 Texture in Nickel Electrodeposition	2
1.4 Microstructure in Nickel Electrodeposition	3
1.4.1 Epitaxial Region	3
1.4.2 Influence of Electroplating Parameters on Grain Size.....	4
2 Materials and Experimental Procedure.....	5
2.1 Pulse-Electroplating Equipment.....	5
2.2 Substrate Material.....	6
2.2.1 Stainless Steel.....	6
2.2.2 Polyamide Fibers	6
2.3 Experimental Procedure.....	7
2.3.1 The Study of Current Density and Temperature Effect on Obtained Microstructure.....	7
2.3.2 The Study of Nickel Concentration and Current Density Effect on the Obtained Microstructure.....	8
2.4 Experimental Techniques	9
2.4.1 X-Ray Diffraction.....	9
2.4.2 Scanning Electron Microscopy	10
2.4.3 Electron Backscatter Diffraction.....	10
3 Results	11
3.1 Surface Characterization	11
3.1.1 Effect of Temperature and Current Density on As-Deposited Nickel Films	11
3.1.2 Effect of Nickel Sulfamate Concentration and Current Density on As-Deposited Nickel Films	13
3.2 X-Ray Diffraction.....	14
3.2.1 Effect of Current Density and Temperature.....	14
3.2.2 Effect of Nickel Sulfamate Concentration and Current Density.....	17
3.3 Microstructure Analysis.....	20
3.3.1 Inverse Pole Figures.....	20
3.3.2 SEM Images	22
3.3.3 EBSD Orientation Maps	24
3.3.4 Grain Size Determination	29
3.4 Pulse-Electroplating on Sandwich Material	31

4 Discussion	33
4.1 Effect of Current Density and Temperature.....	33
4.2 Effect of Nickel Sulfamate Concentration and Current Density.....	33
4.3 Pulse-Electroplating on Sandwich Material	34
5 Conclusion	35
Future Recommendations.....	36
Reference	37
Appendix: Grain Size Determination	40
Appendix: SEM and EBSD Images.....	Error! Bookmark not defined.

Preface

The purpose of the present work is to investigate the influence of the process parameters involved in the pulse-electroplating process with regard to the formed microstructure.

The project was proposed by Prof. Uta Klement and the entire work was performed at the Department of Materials and Manufacturing Technology at Chalmers University of Technology, Gothenburg, Sweden.

The electroplating was performed using two electrolytic solutions named Electrolyte I and Electrolyte II, respectively.

Electrolyte I was already in place and its chemical composition was only partially known while Electrolyte II was mixed and developed during this thesis work.

We would like to take this opportunity to express our gratitude to all the people who have been helpful during the project. Firstly, our gratitude is addressed to Prof. Uta Klement who provided us with this very exciting project. We thank her for the given time and support. Especially, we are grateful for the help in the investigation techniques and the fact that she has been encouraging us during the project.

Secondly, we would like to thank the following persons who have helped us during the project by introducing us to equipment or by giving us assistance or advice:

Yiming Yao – for the introduction to SEM, Gold-sputtering and Electropolishing equipment.

Eric Tam – for XRD training and help in interpreting the results. Also, for supervising the mixing of Electrolyte II.

Roger Sagdahl – for discussions regarding the functionality of the electroplating equipment.

1 Introduction

1.1 Electrodeposition

For more than two centuries, electrodeposition has been a successful technique for coating substrate surfaces with different metallic materials. Various types of substrate materials can be used in electrodeposition including pure metals, conductive polymeric materials, metal composites and alloys. During the electrodeposition process, the deposition of metal ions on the substrate surface at the cathode is caused by charge transfer between cathode and anode in the electrolyte. The charge transfer in this case is driven by an external electrical circuit (figure 1) [1]. Previously, electrodeposition technique was widely used for providing new surface properties to the substrate such as corrosion-, wear- and erosion resistance and in some cases it was used for decorating purposes. However, due to the advancement in materials engineering, nowadays, electrodeposition can be applied to more specific applications such as tailoring magnetic surfaces and electronic components [2].

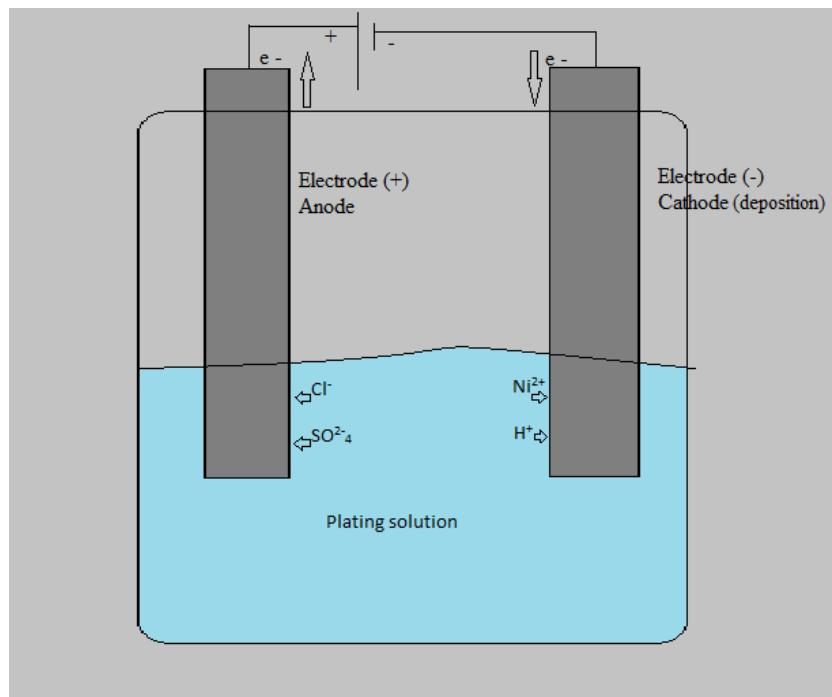


Figure 1: The schematic movement of ions in the electroplating process.

The microstructure of the plated layers is dependent on the various parameters of the electrolyte bath such as bath composition, pH value, temperature, current density, additives, etc. In addition, grain size, texture and internal stress of the substrate can also influence the formation of the electrodeposit [3].

The outstanding performance of the electroplating process like its high production rate with low investment cost makes the process more effective and favorable in the production scale. The porosity-free microstructure is the distinct feature that can be obtained by this technique in the form of thin film coating or free-standing parts [3][4][5][6]. Furthermore, the grain size obtained by performing pulse-electrodeposition

can be below 10 nm. As a result, several properties can be influenced by this change of grain size into nanoscale.

1.2 Electrodeposited Nanocrystalline Structure

Nanostructured material was first introduced by Gleiter [7] as the structure that is formed in non-equilibrium state. When the grains are getting smaller than 100 nm, hardness and wear resistance are increasing due to the large amount of grain boundaries and triple junctions comprising the intercrystalline region. The increase in hardness and yield strength in nanomaterials is in accordance with the Hall-Petch relationship. This behavior is valid down to about 10 nm (depending on material) where an apparent softening occurs which is described by the inverse Hall-Petch relationship. At these small grain sizes, other deformation mechanisms set in [2][4][8]. However, there are also some properties that show no or only a slight dependence on grain size such as Young's modulus, thermal expansion, heat capacity and saturation magnetization [2][8].

Different techniques can be utilized to synthesis nanostructure materials such as sol gel technique, spark erosion, gas condensation, ball-milling and electroplating technique. In the case of electroplating, the nanostructure of as-deposited materials can be obtained by using pulse current instead of direct current [6]. Pulse-electroplating is one of the most attractive techniques due to the distinctive structures obtained by the electrochemical process and the outstanding properties of the nanostructure. The various parameters that influence the nanostructures produced by electroplating technique are now more in the research objective for better understanding in the way how each parameter is involved in the formation mechanism of the nanocrystalline structure [8].

Crystallization of materials occurs with the competition between the nucleation of new grains and the growth of the existing grains. The dominance of either nucleation or growth process is dependent on the processing conditions. In electrodeposition, the nucleation rate can be increased in the condition of high current density (overpotential) and low surface diffusion of ad-atoms of existing grains which results in the achievement of nanostructure. On the other hand, grain growth can occur in the condition of low current density (overpotential) and high surface diffusion [2][3].

Generally, the microstructure produced by electrodeposition is influenced by the bath conditions. However, in the very first layer of the deposited film, epitaxial grains can be found which are influenced by the crystallographic structure of the substrate rather than the bath conditions. This layer is formed for only a few microns. When the film layer becomes thicker, the grains will grow in a preferred orientation depending on the bath conditions [9][10].

1.3 Texture in Nickel Electrodeposition

According to Amblard et al. [10], two important theories have been used to describe the anisotropy of the texture of Nickel electrodeposit which are explained from the opposite viewpoints. One theory says that the competition in nucleation is responsible for the anisotropy while the theory one suggests that it is the competitive growth that determines the anisotropy. However, the literature data have shown that both theories are insufficient to fully describe all experimental results.

Pangarov [9] suggested that the anisotropy of the texture of Nickel electrodeposit is dependent on the nucleation process which is related to the overpotential. As mentioned by Pangarov, the possible textures of the metals with fcc structure when increasing overpotential are $\langle 111 \rangle$ - $\langle 100 \rangle$ - $\langle 110 \rangle$ - $\langle 311 \rangle$ - $\langle 210 \rangle$ [9]. However, this theory can be explained only in the pure condition which means that neither the influence of defects on the substrate surface nor the adsorption of other species in the electrolyte is considered. However, in reality, metallic surfaces are usually not defect-free. Additionally, for the transition materials with high surface energy such as Nickel, it is less likely that it does not contain any adsorbed species. This means, the conditions are then considered to be unrealistic [10].

Opposite to Pangarov's theory, other authors state that the anisotropic texture of the Nickel electrodeposit is determined by the growth process. In this way, the hydrogen adsorption (H_{ads}) becomes an important factor for controlling the texture during electrodeposition. When the level of H_{ads} increases, the texture develops from $\langle 110 \rangle$ to $\langle 100 \rangle$ and finally $\langle 200 \rangle$. Although this theory includes the consideration of the H_{ads} influence on the film texture, it is insufficient to explain all the possible preferred orientations of the Nickel electrodeposit. This is due to the fact that H_{ads} is not the only species in the electrolyte that could inhibit the growth of the Nickel crystals [10][11].

In an additive-free bath, the $\langle 110 \rangle$ -texture is the inhibition growth mode influenced by H_{ads} while the $\langle 211 \rangle$ -texture is the result of the presence of $Ni(OH)_2$. Also, $\langle 210 \rangle$ -texture is affected by Hydrogen gas in the electrolyte. The growth of the $\langle 100 \rangle$ -texture cannot be related to any inhibiting species and this is why this texture is considered as the free growth mode. Each type of species can be linked to the pH value of the electrolyte. Hence, the presence of a texture at a specific pH value and current density can be predicted as in the diagram presented by Amblard et al. [10].

In pulse-electrodeposition, the adsorption and desorption of inhibitors on the substrate surface can be hindered by the T_{on} - (plating time) and T_{off} -time (relaxation time) which provide the possibility of creating deposit with better properties [12]. Molecular inhibitors will desorb from the substrate surface during the relaxation period (T_{off}) while H_{ads} and anions behave contrarily, i.e. they will adsorb to the interface and inhibit the growth of the Nickel coating on the surface. The perturbation that is dependent on the frequency and duty cycle of the electroplating system plays an important role in determining the characteristics of the Nickel electrodeposit. A small perturbation level provides less structural defects with larger grain size, while at high perturbation, $\langle 110 \rangle$ growth mode is dominant for all kinds of inhibiting species. This is due to the inhibition of H_{ads} which becomes the only factor governing the growth of the Nickel electrodeposit [12].

1.4 Microstructure in Nickel Electrodeposition

1.4.1 Epitaxial Region

The epitaxial layer is a very fine-grained layer formed next to the substrate surface with the same structure and grain orientation as the substrate material. The main advantage of this layer is to reduce the interfacial energy between the substrate and the electrodeposited layer. The difference in lattice constants between substrate and deposited materials results in the occurrence of a misfit strain in the epitaxial layer. This leads to a high dislocation density in order to accommodate the misfit strain. A tolerable strain supported by the

microstructure can be up to 12%. Experimental results of the previous literature showed that the thickness of the epitaxial layer of electrodeposited Nickel on a Cu substrate can reach up to 100 nm before the columnar grains with no orientation relationship to the substrate are formed [13].

1.4.2 Influence of Electroplating Parameters on Grain Size

The various parameters involved in the Nickel electrodeposition have been studied for revealing the relation with the microstructure in order to improve the process of synthesizing nanostructured Nickel [6][14][15][16][17][18]. Although the nanostructured Nickel have already been produced, the tailoring of Nickel electrodeposit properties is still complex. This is due to the uncertain results when the effects of all plating parameters are involved.

Compared with the direct current (DC) electroplating [19][20], the on-time and off-time intervals in pulse-electroplating have a significant influence on the microstructure of the Nickel electrodeposit. The longer on-time and higher current density is applied, the smaller grain size down to a few nanometers can be produced. The higher number of duty cycle initiate more nucleation sites for Nickel crystals on the substrate and leads to the smaller grain size. According to Ravi et al. [20], the grain size linearly decreases with the higher number of duty cycle.

For the influence of current density on the grain size, the results are still controversial in different studies. According to Rashidi [21], in pulse-electroplating process, the grain size can be decreased with an increase in current density but the effect is just substantial up to 7.5 A/dm². After that, a further increase in the current density will not influence the grain refinement to the same extent. This finding is in contrast to some experiments [14][15][18] on DC electroplating of Nickel where the grain size linearly increases with increasing the current density.

The effect of temperature on the grain morphology is still not generally identified. However, it is accepted that the deposition rate, coating quality and some other properties can be altered with only small variations in bath temperature [22]. From the results proposed by Rashidi [21], the grain size of electrodeposits will increase when the bath temperature increases. But this behavior is only valid for temperatures above 55 °C. This observation is also in accordance with the diagram introduced by Dini [23] and the study on nanocrystalline electrodeposits by Natter et al. [24].

Additionally, the grain size of the electrodeposited materials is also dependent on other parameters such as the frequency and the concentration of bath additives like saccharin which acts as a grain refiner.

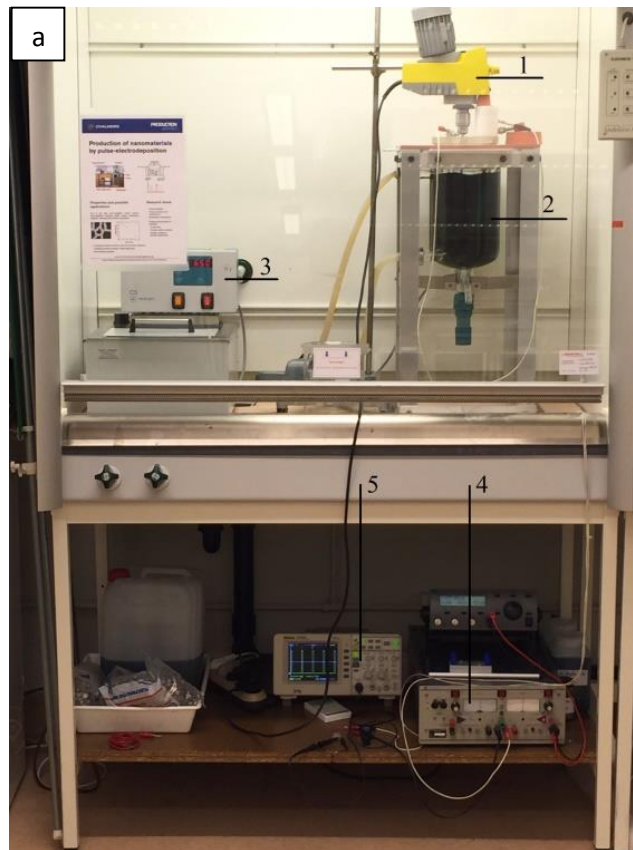
2 Materials and Experimental Procedure

The experimental section of the current thesis work had three objectives: (1) Production of materials with nanocrystalline microstructure by adjusting the process parameters. (2) Characterization of the electrodeposited materials. (3) Deposition of a Nickel coating on polymer fibers in a sandwich structure and investigation of the coating quality.

2.1 Pulse-Electroplating Equipment

All samples were produced in the pulse-electroplating equipment illustrated in figure 2. The equipment contains the following parts:

1. Propeller
2. Plating bath of 2 liters
3. Heating device for warming the electrolyte to the required temperature
4. Pulse generator
5. Oscilloscope for reading the current parameters



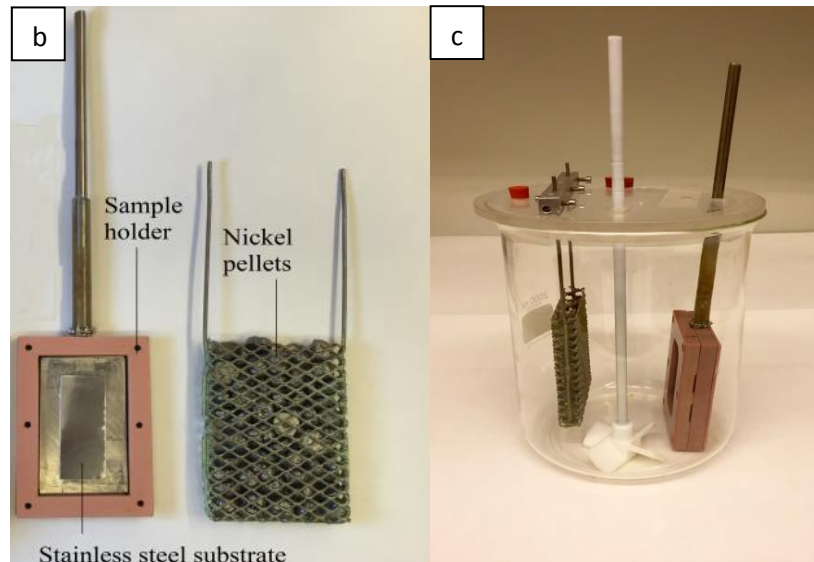


Figure 2: Pulse-Electroplating equipment: a) Overview of the equipment, b) anode and cathode, i.e. sample holder and basket with Nickel pellets, and c) set-up of cathode, anode and propeller.

2.2 Substrate Material

2.2.1 Stainless Steel

As substrate material, a stainless steel plate of 30 mm * 60 mm * 1.5 mm was used. The stainless steel had the advantage that the Nickel coating could be easily stripped off afterwards.

No mechanical preparation of the substrate was required before the electrodeposition process. However, a cleaning and degreasing operation was performed. The substrate was rinsed both under tap water and by ethanol and afterwards blow-dried in order to avoid stains.

After the electrodeposition process, the coated layers were removed from the sample holder and cleaned. This means, the electrodeposited films were rinsed under distilled water and subsequently by ethanol. To avoid stains, the coated samples were cleaned for 5 or 10 minutes in an ultrasonic bath containing ethanol and afterwards blow-dried.

2.2.2 Polyamide Fibers

A set of experiments was performed in order to investigate if a Nickel electrodeposit could be applied to strengthen the Hybrix™ sandwich material produced by *Lamera AB*. The material investigated consisted of stainless steel plates between which Polyamide 6.6 fibers were attached with help of an Epoxy adhesive. The cross section of the sandwich material can be seen in figure 3. Since the Polyamide fibers are not conductive, Gold sputtering was chosen to create a conductive layer on the fibers. The process was performed using an Edwards Sputter Coater S150B where the process was carried out at 1 kV within five minutes.

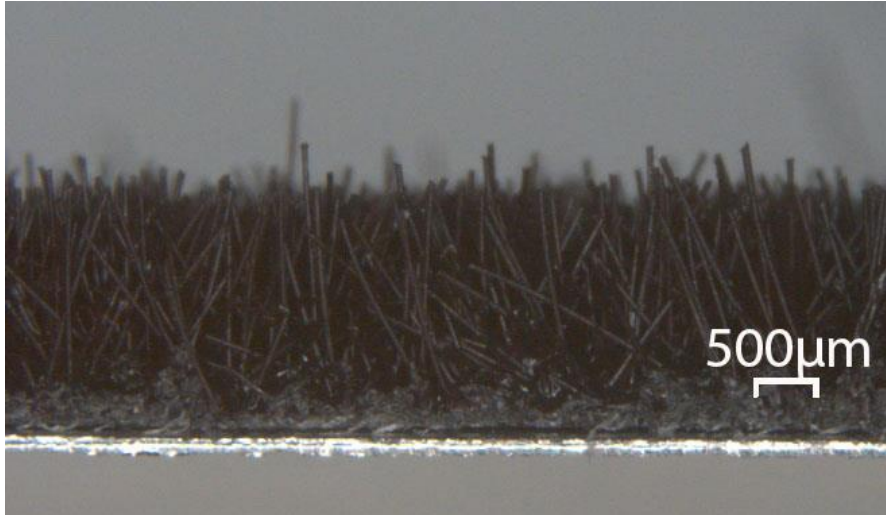


Figure 3: Cross section of the composite material showing the bottom steel plate and the attached fibers. The top steel plate is missing to facilitate Gold-sputtering.

2.3 Experimental Procedure

The intended experiments were performed by using two different electrolytic baths, an existing electrolyte (Electrolyte I) and a newly mixed electrolyte (Electrolyte II). The chemical composition of each electrolyte will be described later-on in this section.

2.3.1 The Study of Current Density and Temperature Effect on Obtained Microstructure

In this study, Electrolyte I was used to produce the samples for studying the effect of current density and temperature on Nickel electrodeposit. The electrolyte contains Nickel Sulfamate as the main ingredient and has a pH value in the range of 3 to 5 (see Appendix). The solution is additive-free and contains Boric acid, Magnesium Chloride and Natrium Citrate.

A set of experiments was performed at different current densities, i.e. 2, 10 and 20 A/dm². In addition to the current density, also temperature was varied between 35°C and 75°C with a step size of 10 degrees. This resulted in 15 samples where five different temperatures were used at each of the three current density value as shown in table 1.

Table 1: List of the conditions used for studying the current density and temperature effect on Nickel electrodeposit.

Current Density (A/dm ²)	Temperature (°C)
2	35
	45
	55
	65
	75
10	35
	45
	55
	65
	75
20	35
	45
	55
	65
	75

2.3.2 The Study of Nickel Concentration and Current Density Effect on the Obtained Microstructure

Electrolyte II was used to produce the samples for studying the effect of Nickel Sulfamate concentration and current density on the formed microstructure. The electrolyte contains a substantial amount of Nickel Sulfamate ($\text{Ni}(\text{SO}_3\text{N}_2) \cdot 4\text{H}_2\text{O}$) as the main source of Nickel ions. In addition, Boric acid (H_3BO_3) and Magnesium Chloride were added. The solution was continuously developed to investigate the influence of the Nickel Sulfamate concentration on the appearance and microstructure of the electrodeposits. The initial chemical composition of the electrolyte is stated in table 2 and the development of the electrolyte is shown in table 3. Also, the conditions used for producing the samples are displayed in table 4.

Table 2: The initial chemical composition of Electrolyte II showing the concentration of Nickel Sulfamate in Molar [M].

Chemical Component	Nickel Sulfamate $\text{Ni}(\text{NH}_2\text{SO}_3)_2$ [M]	Boric Acid H_3BO_3 [g]	Magnesium Chloride MgCl_2 [g]	Sodium Citrate $\text{C}_6\text{H}_5\text{Na}_3\text{O}_7$ [g]	Water H_2O [L]
Amount	0.75	81.16	11.71	19.01	0.98

Table 3: The development of Nickel Sulfamate concentration in Electrolyte II.

Chemical Component	1st Concentration	2nd Concentration	3rd Concentration	4th Concentration	5th Concentration	6th Concentration
Nickel Sulfamate $\text{Ni}(\text{NH}_2\text{SO}_3)_2$ [M]	0.75	1.75	1.85	2.15	2.44	2.89

Table 4: List of the conditions used for studying the Nickel Sulfamate concentration and current density effect on the formed microstructure.

Nickel Sulfamate Concentration (Molar)	Current Density (A/dm^2)
1.85	2
	10
	20
2.15	2
	10
	20
2.44	2
	10
	20
2.89	2
	10
	20

2.4 Experimental Techniques

For investigation of the microstructure changes (i.e. grain size, texture, grain size distribution, and surface topography) that take place when changing the process parameters, different advanced characterization techniques were used.

2.4.1 X-Ray Diffraction

X-ray diffraction (XRD) is used to determine the interplanar spacing of crystalline materials which provide information about the phase composition, residual stresses and atomic structure. It also gives an impression about the overall texture when the diffractogram is compared to that of a powder standard (which has a random texture and is found in the database).

The working principle is based on a monochromatic X-ray beam which irradiates the sample (under various angles Θ) while the XRD detector is rotating and measures the intensity of the diffracted beam as a function of 2Θ (Θ is the diffracted angle). The information is collected, plotted and then compared to the data found in the database. [25].

Investigations were performed by a Bruker D8 Advance X-ray diffractometer using a Cr-anode (wavelength = 2.28970 Å) and a generator power of 35 kW and 40 mA. The angle Θ was varied in the range of 65° to 140°. All samples were scanned at room temperature for about 6 minutes each.

No sample preparation was required apart from that the samples were cut to a length of 40 mm in order to fit into the sample holder.

2.4.2 Scanning Electron Microscopy

In Scanning Electron Microscopy (SEM), an electron beam scans the sample surface and as a result, various signals can be obtained such as backscattered electrons, secondary electrons, and characteristic X-rays, which can be used for imaging and chemical analysis.

2.4.3 Electron Backscatter Diffraction

Electron Backscatter Diffraction (EBSD) is a technique that provides microstructural and crystallographic information, e.g. local texture, grain morphology, grain boundary distribution, grain size and grain size distribution [26]. The technique is able to inspect a considerable amount of grains in a relatively short period of time. The EBSD detector is an attachment to the SEM. With the cooperation of the required evaluation software, it can be used to measure and identify electron backscattered diffraction patterns (EBSP or Kikuchi patterns). To obtain so-called orientation map, a color-coded representation of the grains in the microstructure, the sample is tilted 70° towards the EBSD detector in the SEM and a defined area is scanned with a suitable step size (depending by the grain size). At each point (pixel), an EBSP is captured with a CCD (Charge Coupled Device) camera and the software indexes the obtained pattern by comparing it with the crystallographic data of the expected phase which has to be selected before the investigation. A specific color is addressed to the pixel which represents the measured orientation. In case that indexing was not possible as a result of undefined phase, overlapping patterns from adjacent grains or due to poor pattern quality, the pixel will be referred to as “zero solution”.

In this thesis work, the samples were investigated using a Leo 1550 Gemini FEG-SEM equipped with a Nordlys II EBSD detector and Channel 5 software by HKL Technologies. Afterwards, the obtained data was analyzed further by Channel 5 software with respect to grain size distribution in order to obtain pole figures and inverse pole figure diagrams.

Prior to EBSD analysis, the samples were prepared by electropolishing. A Struers LectroPol-5 device with a Struers A2 electrolyte consisting of 70% Perchloric acid and 30% 2-Butoxyethanol was used for 10 seconds at a voltage of 31 V. The size of the electropolished samples was around 1 cm. After electropolishing, the samples were rinsed with Ethanol and placed in water for ending the corrosion process before they were blow-dried.

3 Results

3.1 Surface Characterization

3.1.1 Effect of Temperature and Current Density on As-Deposited Nickel Films

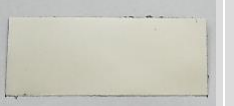
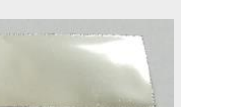
Based on the experiments, all the produced samples show a bright or semi-bright surface where the degree of brightness differs in each sample depending on the plating condition. In the temperature range between 55°C to 75°C, the as-plated Nickel films tend to have duller surface when the current densities decrease. However, when produced at 35°C, the films are shinier when the current density is decreased. In the case of a bath temperature of 45°C, the sample with the best appearance was produced at 10 A/dm². In general, at all current densities, the Nickel coatings tend to become duller when the bath temperature is decreased except for the sample produced at 35°C with 2 A/dm² current density that shows a really bright-shiny surface.

Waviness on the surface can be found in the samples produced at low plating temperature. However, the waviness disappears when the current density is decreased (figure 5). Pitting is another defect that can be observed in this study (figure 6). It is usually found at moderate plating temperatures and its size is smaller when the current density decreases. The thickness of the film obviously varies with the current density. When using the same deposition time, the film thickness increases with the increase in current density. The appearance of the produced samples is summarized in table 5 and 6.

Table 5: The effect of current density and temperature on the appearance of Nickel electrodeposits.

Temperature Current Density	35 °C	45 °C	55 °C	65 °C	75 °C
2 A/dm ²	B - -	B - -	B - -	B - -	B - -
10 A/dm ²	D - W	B P -	B P -	B - -	B - -
20 A/dm ²	D - W	D P W	B P -	B - -	B - -
Description :	1st line-----> [Bright = B, Dull = D] 2nd line-----> [Pitting = P] 3rd line-----> [Wavy = W]				

Table 6: The surface appearance of Nickel electrodeposits produced by varying current density and temperature.

Temperature Current Density	35 °C	45 °C	55 °C	65 °C	75 °C
2 A/dm ²					
10 A/dm ²					
20 A/dm ²					

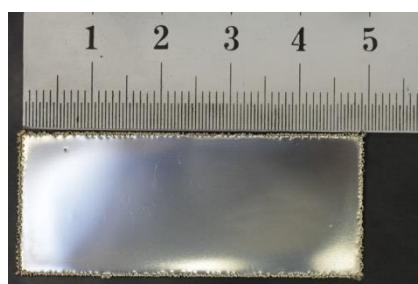


Figure 4: Bright and smooth surface of the sample produced at 20 A/dm² and 65 °C.



Figure 5: Waviness of the sample produced at 20 A/dm² and 35 °C.



Figure 6: Pitting observed in the sample produced at 20 A/dm² and 45 °C.

3.1.2 Effect of Nickel Sulfamate Concentration and Current Density on As-Deposited Nickel Films

The appearance of the samples produced with Electrolyte II is very different from those produced with Electrolyte I (figure 7). The distinct appearance of these films is the very thin dark layer on the surface that can be observed in all samples. The degree of the brightness varies with the Nickel Sulfamate concentration and also the current density. With the increase in Nickel Sulfamate concentration, the brightness of the films gradually increases. It can also be noticed that the films gets brighter when the current density increases. It is observed that the dark thin layer on the film surface is very sensitive to grease and oil. When touching the samples with bare hands, stains easily show up and they are hard to remove. It is also noticed that this layer has a sensitive surface, i.e. that it can easily be scratched even by a plastic tool. The appearances of the samples produced in this study are summarized in table 7.

Table 7: The surface appearance of Nickel electrodeposits produced by varying current density and Nickel Sulfamate concentration.

Nickel Sulfamate Concentration	Current Density		
	2 A/dm ²	10 A/dm ²	20 A/dm ²
1.85 M			
2.15 M			
2.44 M			
2.89 M			



Figure 7: Comparison of the appearance of the samples produced under the same plating condition with Electrolyte I (Top) and Electrolyte II (Bottom).

3.2 X-Ray Diffraction

3.2.1 Effect of Current Density and Temperature

In table 8, the results of XRD measurements for the current densities of 2 A/dm², 10 A/dm² and 20 A/dm² are shown. The information contained in the table consists of the intensity values observed for {111}- and {200}-reflections. Additionally, texture coefficient and the grain size as obtained by Scherrer equation are also shown in the table. The Scherrer equation is shown in the formula below.

$$\tau = \frac{K\lambda}{\beta \cos\theta}$$

τ = the average grain size

K = shape factor

λ = X-ray wavelength

β = half the maximum intensity (FWHM)

θ = the Bragg angle

The intensity of both {111}- and {200}-reflections increase when the current density increases. The variation in peak intensity values and texture coefficient of the samples produced with different conditions can be seen in table 8. However, XRD patterns of all samples are the same in all conditions. Representative diffractograms of the samples from this experiment are shown in figure 8 and 9.

Table 8: Summary of XRD data of the analyzed Nickel electrodeposits showing the intensity in {111} and {200} plane, texture coefficient, and grain size calculated by using Scherrer equation.

Current Density	Temperature	{111} Reflection Intensity	{200} Reflection Intensity	Texture Coefficient ($I_{\{200\}}/I_{\{111\}}$)	2θ	FWHM	Grain Size by Scherrer Equation (nm)
2 A/dm²	35 °C	695	3311	4,76	81,10	0,818	19,00
	45 °C	659	5668	8,60	81,00	0,666	23,31
	55 °C	677	5964	8,81	81,05	0,612	25,38
	65 °C	612	4946	8,08	81,10	0,753	20,64
	75 °C	586	4225	7,21	81,10	0,756	20,55
10 A/dm²	35 °C	451	7639	16,94	81,01	0,682	22,77
	45 °C	785	3626	4,62	81,00	0,904	17,18
	55 °C	749	4090	5,46	81,00	0,817	19,01
	65 °C	648	6865	10,59	81,10	0,675	23,02
	75 °C	543	6694	12,33	81,10	0,696	22,33
20 A/dm²	35 °C	642	9295	14,48	81,11	0,409	38,00
	45 °C	381	6477	17,00	81,00	0,586	26,50
	55 °C	853	3615	4,24	81,11	0,865	17,96
	65 °C	781	4339	5,56	81,00	0,733	21,18
	75 °C	669	6619	9,89	81,00	0,749	20,73

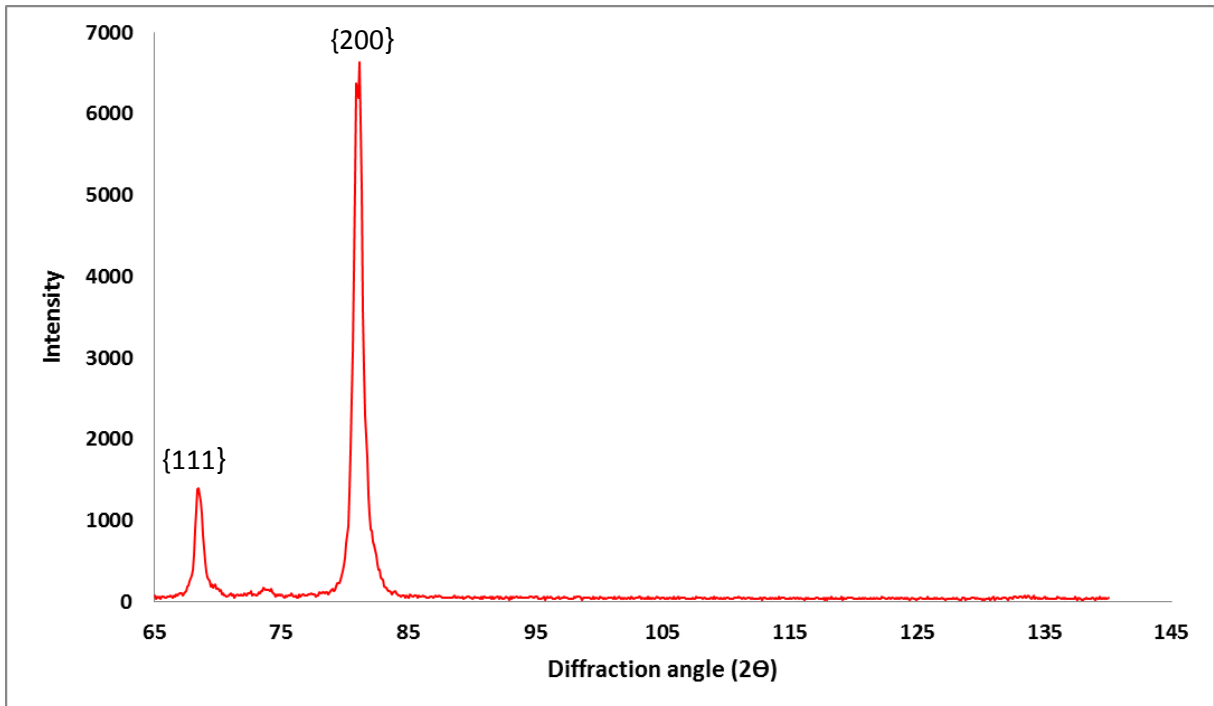


Figure 8: XRD pattern of an electrodeposit produced at 2 A/dm² and 35°C.

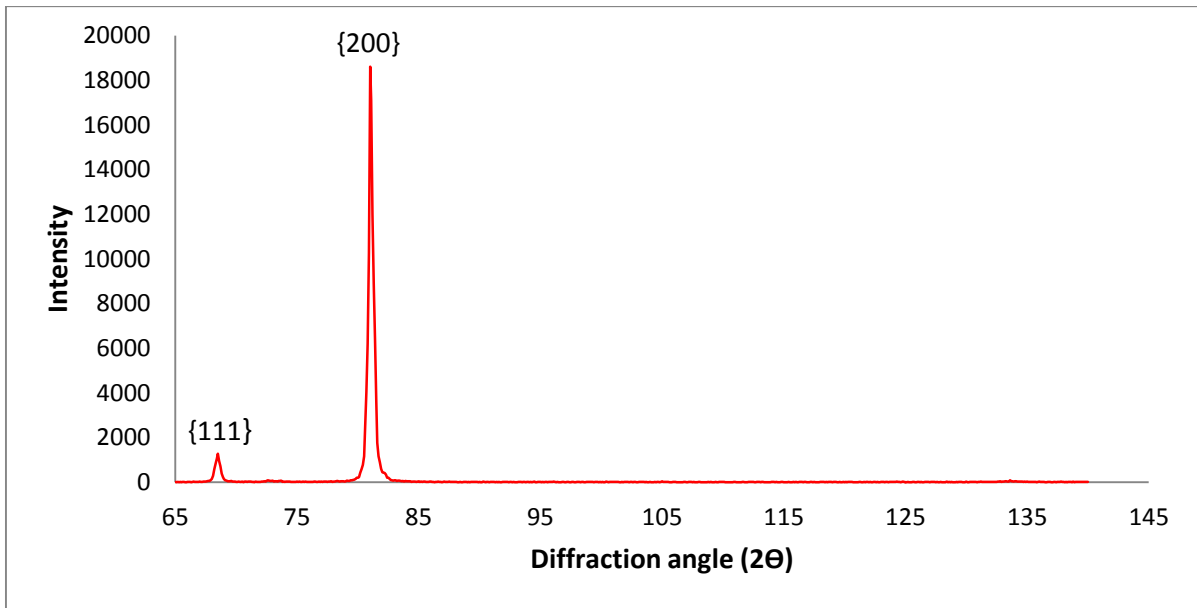


Figure 9: XRD pattern of an electrodeposit produced at 20 A/dm² and 35°C.

A representative XRD pattern of the samples was plotted in comparison with the XRD pattern of Nickel powder (figure 10 and 11). The XRD patterns of Nickel electrodeposits show a very strong intensity in {200} reflection, while the {220} reflection is not present on the XRD profiles. The difference in XRD patterns between Nickel electrodeposits and Nickel powder indicates that Nickel electrodeposits have a certain texture (Nickel powder is considered to have a random texture).

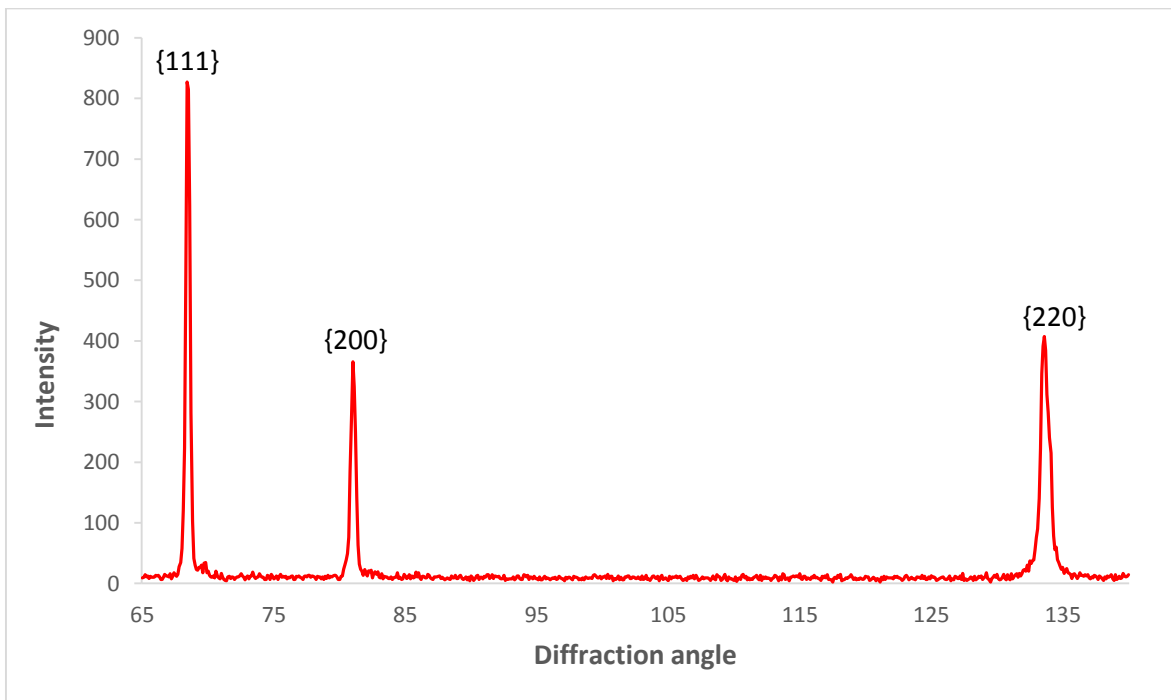


Figure 10: XRD pattern of Nickel powder.

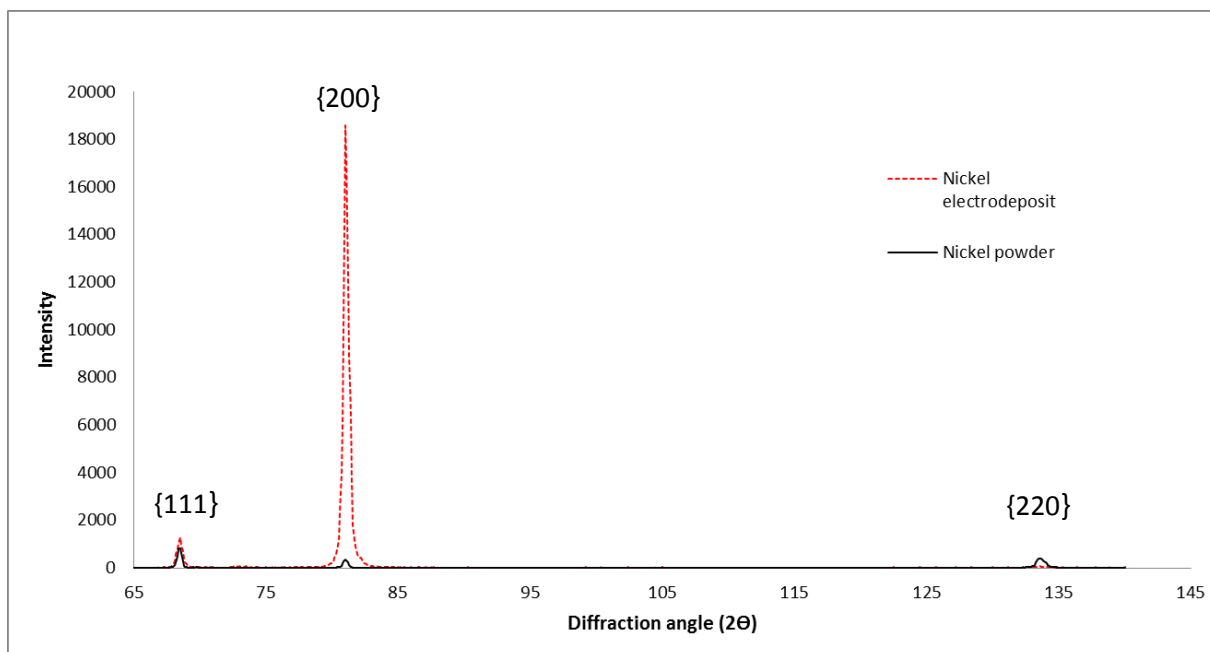


Figure 11: Comparison of XRD patterns of as-deposited Nickel and Nickel powder.

3.2.2 Effect of Nickel Sulfamate Concentration and Current Density

Table 9 provides the XRD data collected from electrodeposits produced with Electrolyte II. In addition to intensity values observed for {111} and {200} reflections, also data for the {220} reflection are included. Additionally, texture coefficient and the grain size obtained by Scherrer equation are provided in table 9. The schematic plots of two different XRD patterns of the samples produced in this study are exhibited in figure 12 and 13. The samples produced at 2 A/dm² show a higher value of {111} peak intensity while the samples produced at 20 A/dm² reveal a higher {220} peak.

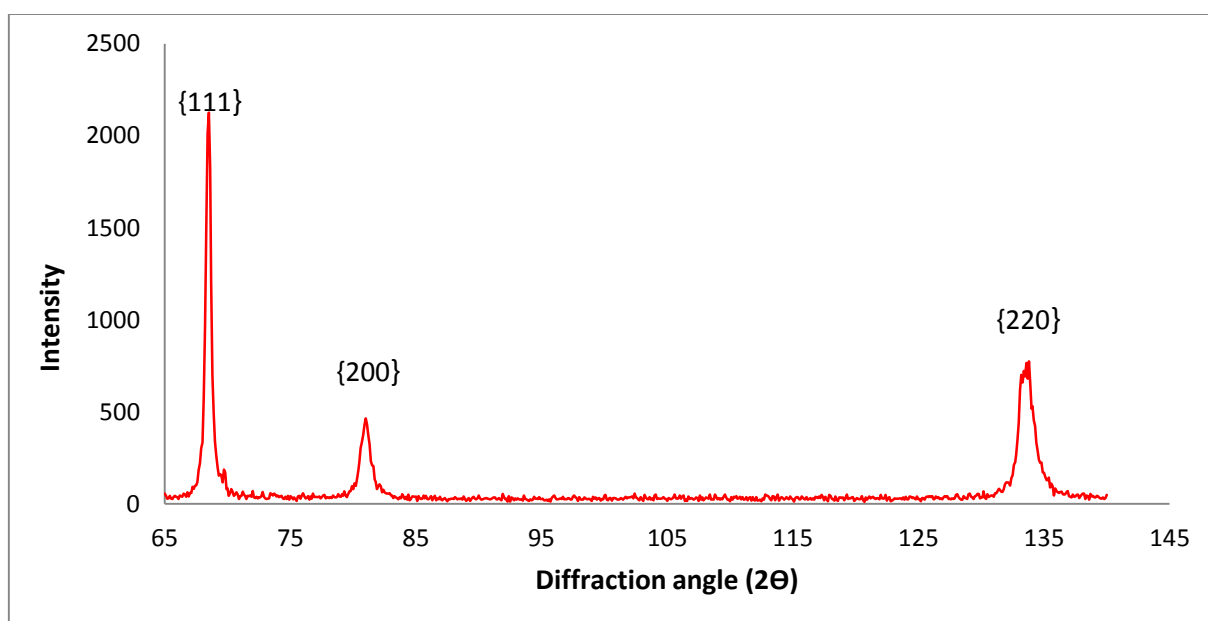


Figure 12: XRD profile of the sample produced at 2 A/dm² and 2.44 M of Nickel Sulfamate concentration showing the highest intensity in the {111} peak.

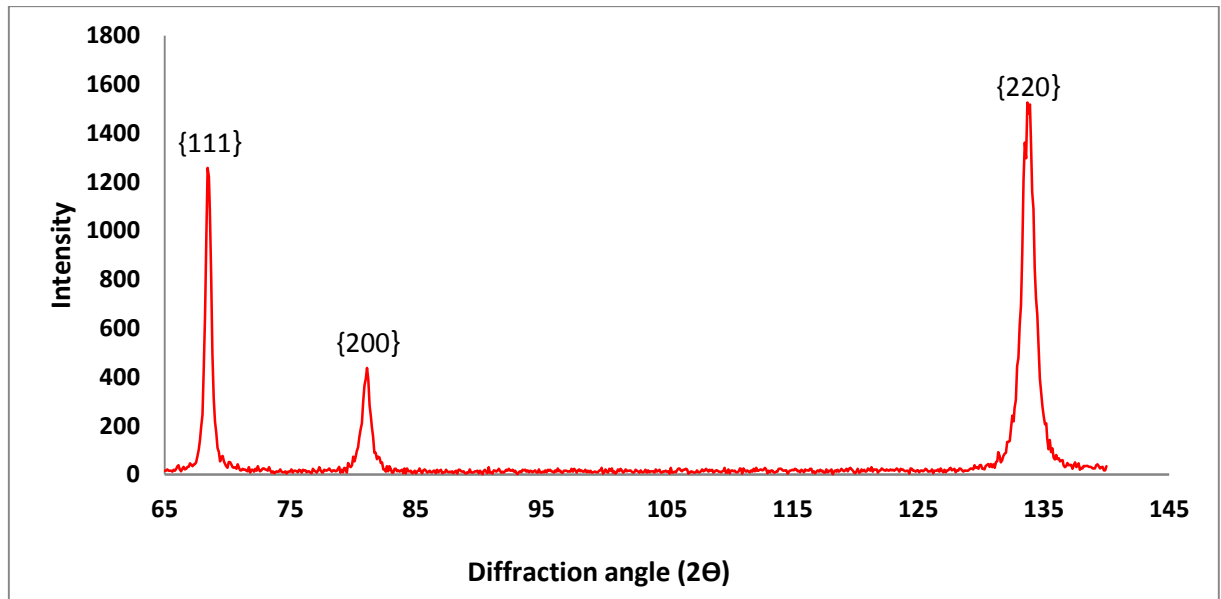


Figure 13: XRD profile of the sample produced at 20 A/dm² and 2.44 M of Nickel Sulfamate concentration showing the highest intensity in the {220} peak.

Table 9: XRD data collected from the samples produced by varying current density and Nickel Sulfamate concentration.

Nickel Sulfamate Concentration	Current Density	{111} Reflection Intensity	{200} Reflection Intensity	{220} Reflection Intensity	Texture Coefficient ($I_{(200)}/I_{(111)}$)	2θ	FWHM	Grain Size by Scherrer Equation (nm)
1.85 M	2 A/dm ²	-	-	-	-	-	-	-
	10 A/dm ²	714	211	516	0,30	68,40	0,624	22,88
	20 A/dm ²	722	187	706	0,26	68,50	0,567	25,19
2.15 M	2 A/dm ²	964	220	322	0,23	68,40	0,534	26,73
	10 A/dm ²	804	191	556	0,24	68,50	0,569	25,10
	20 A/dm ²	735	218	743	0,30	133,80	1,254	24,00
2.44 M	2 A/dm ²	1064	232	387	0,22	68,50	0,510	28,01
	10 A/dm ²	784	199	616	0,25	68,50	0,521	27,42
	20 A/dm ²	628	220	762	0,35	133,70	1,140	26,34
2.89 M	2 A/dm ²	1053	241	474	0,23	68,41	0,536	26,63
	10 A/dm ²	710	248	712	0,35	133,81	1,175	25,62
	20 A/dm ²	624	214	931	0,34	133,71	1,125	26,70

The increase in current density enhances the dominance of {220} reflection in XRD at all Nickel Sulfamate concentrations as can be seen in figure 14. Additionally, with the higher concentration of Nickel Sulfamate in solution, a slight increase in each peak intensity can be observed (table 9).

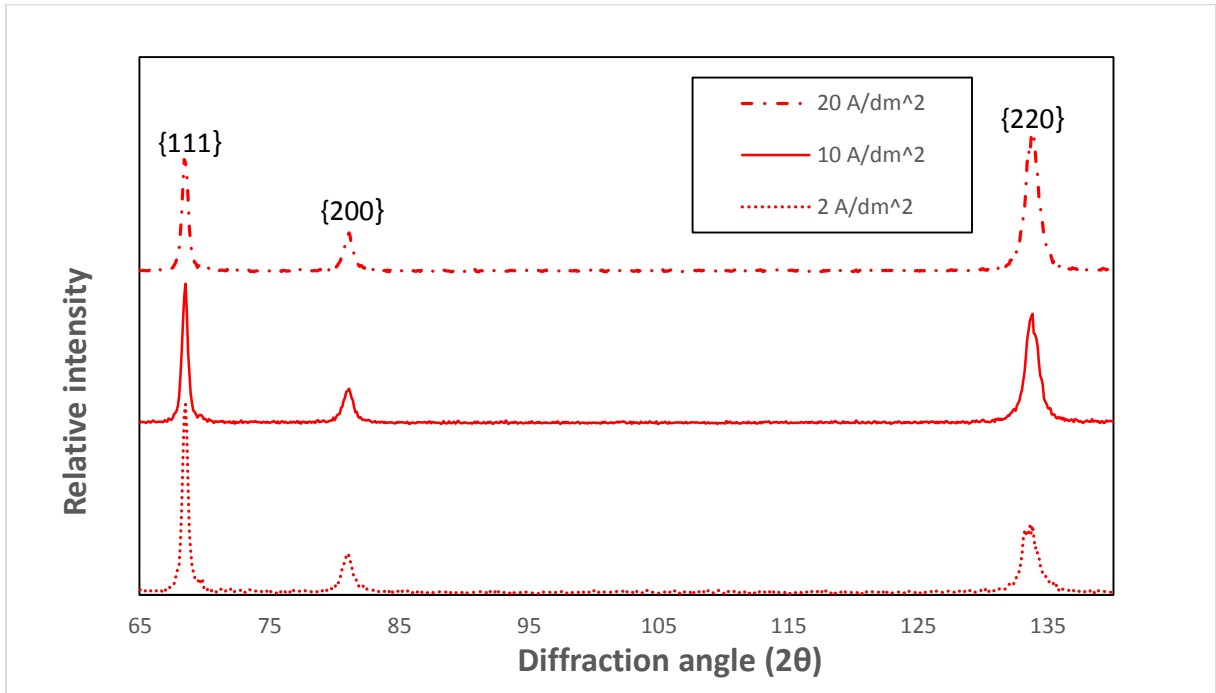


Figure 14: The effect of current density on {111} and {220} peak in XRD profiles of the samples produced at 2.44 M of Nickel Sulfamate concentration.

Both XRD patterns of the samples produced in this study were compared to the XRD pattern of Nickel powder to investigate the existence of the texture in the produced microstructures. The schematic plots of the comparisons can be seen in figures 15 and 16. The difference in XRD patterns between as-deposited Nickel films and Nickel powder demonstrates the development of texture in the microstructures of the samples produced in this study.

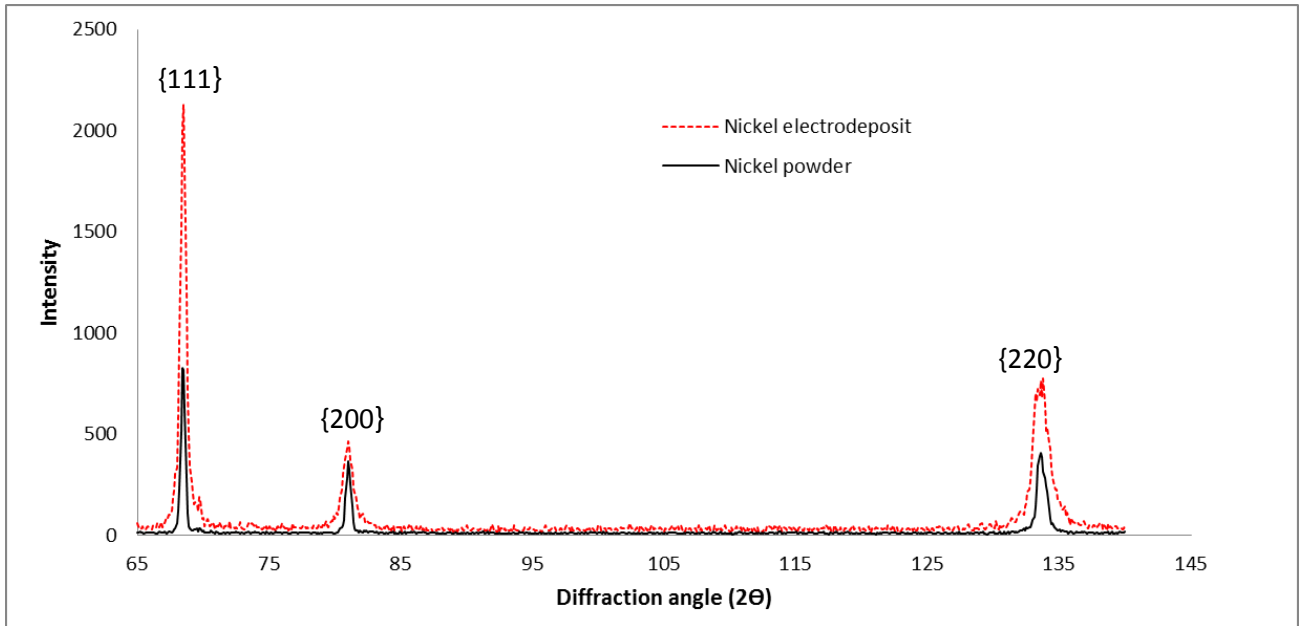


Figure 15: Comparison of XRD patterns of the as-deposited Nickel film produced at 2 A/dm² and Nickel powder.

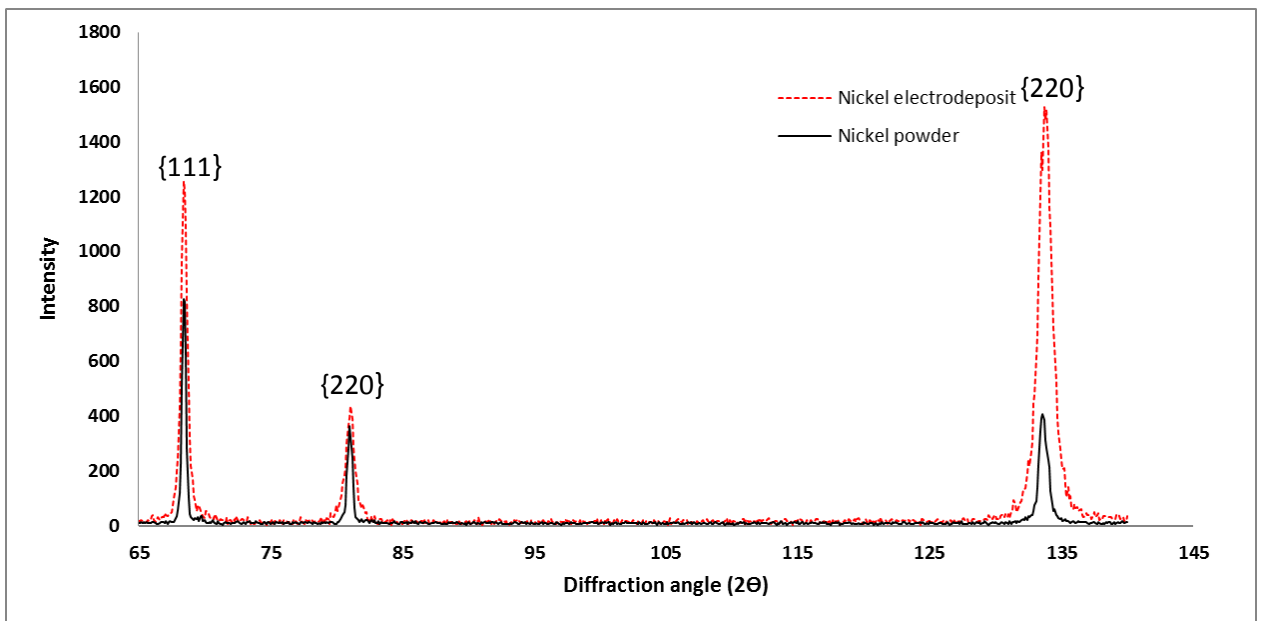


Figure 16: Comparison of XRD patterns of the as-deposited Nickel film produced at 20 A/dm² and Nickel powder.

3.3 Microstructure Analysis

3.3.1 Inverse Pole Figures

Inverse pole figures were plotted from the data obtained by EBSD. These are used for analyzing the crystallographic orientation in the microstructure of the as-deposited Nickel films. In all cases, the growth direction is parallel to the Z axis. Contouring is applied with the setting of half width at 10° and the data clustering limit is 3°.

Regarding the information of the samples produced with Electrolyte I, texture is not influenced by the change in temperature and current density. All the as-prepared samples show a strong preferred orientation of $\langle 100 \rangle$ in the growth direction. A representative inverse pole figure of the samples is shown in figure 17.

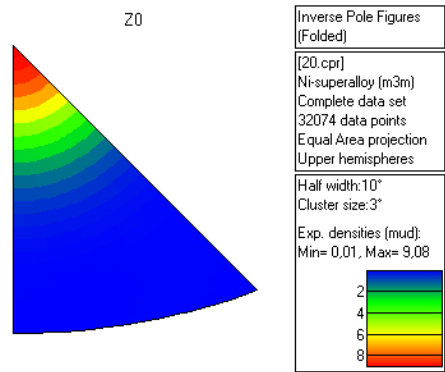
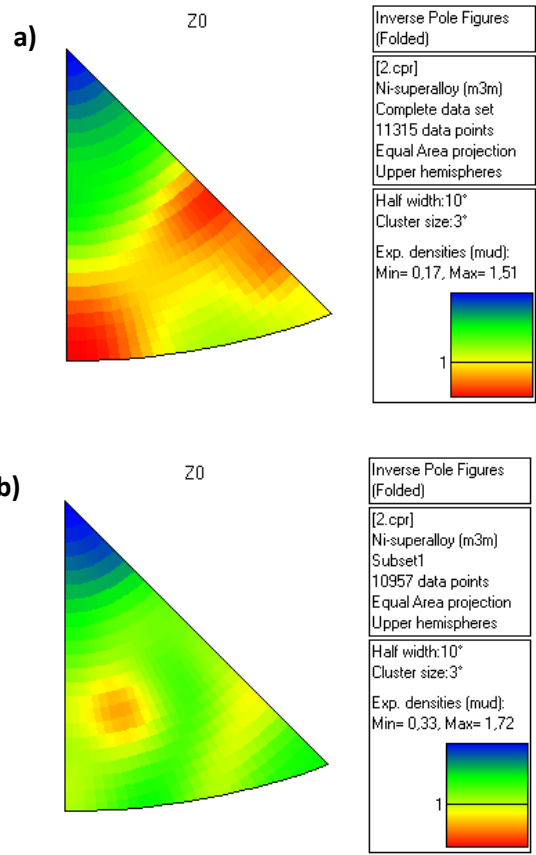


Figure 17: Inverse pole figure of sample being representative for all samples produced with Electrolyte I.

The samples produced with Electrolyte II at 2 A/dm² with different Nickel Sulfamate concentrations show a random texture (figure 18). In contrast, as-deposited Nickel films produced at 20 A/dm² with different Nickel Sulfamate concentrations show a weak $\langle 110 \rangle$ -texture parallel to the growth direction (figure 19).



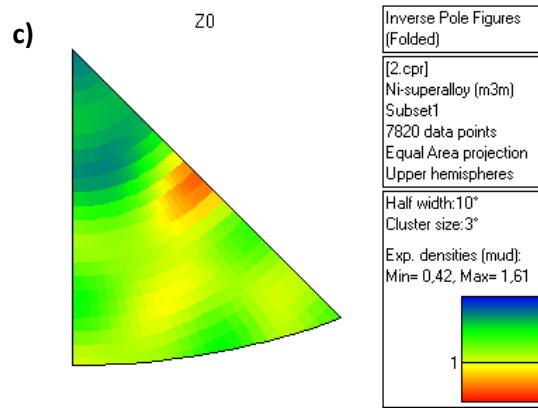


Figure 18: Inverse pole figures of the samples produced with Electrolyte II at 2 A/dm² with Nickel Sulfamate concentration of a) 2.15M b) 2.44M and c) 2.89M.

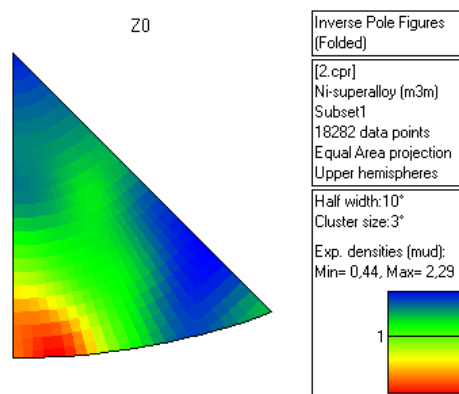


Figure 19: Inverse pole figure of the sample produced with Electrolyte II at 20 A/dm² with Nickel Sulfamate concentration of 2.89 M.

3.3.2 SEM Images

SEM images were obtained by Forward Scattered Diffraction (FSD) detector. The images illustrate the impression of topography of the microstructures. All samples were observed in top view, i.e. in the growth direction of the grains.

All samples were investigated at the same magnification at 10k to compare the characteristic of the microstructure at different plating conditions. The samples produced with Electrolyte I at 20 A/dm² in bath temperature of 35°C and 45°C reveal the microstructures consisted of big grains with asymmetric shape distributed randomly in a matrix of small grains (figure 20a and 20b). While the samples produced in high bath temperature with different current densities display fine grains well distributed all over the area of investigation. A representative SEM image of fine grain samples is shown in figure 21.

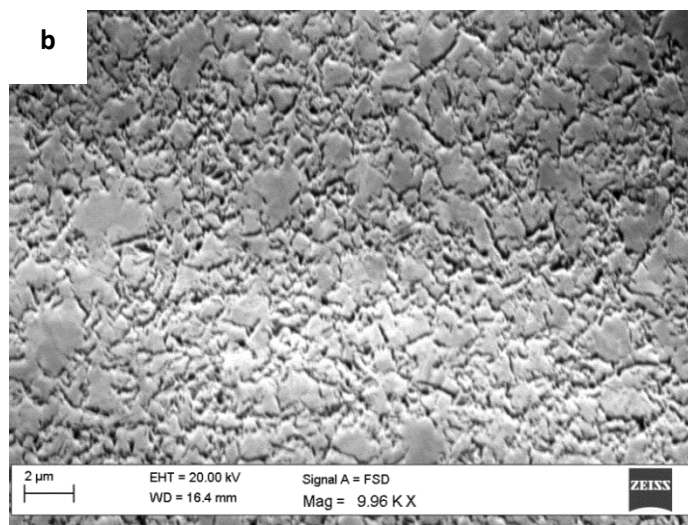
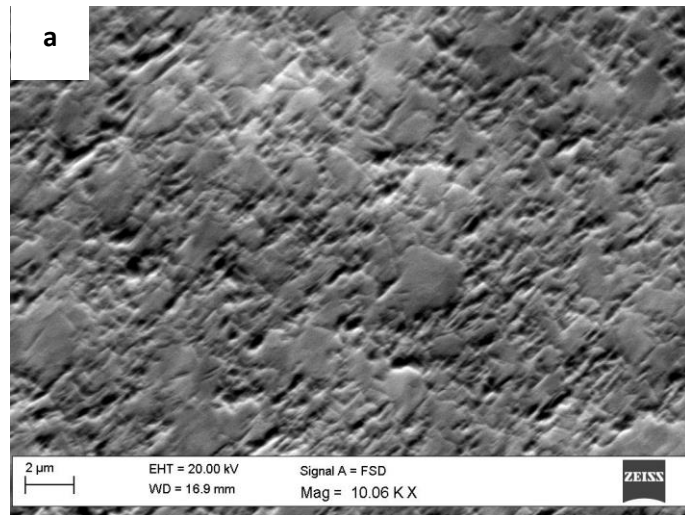


Figure 20: SEM images of samples produced with Electrolyte I at 20 A/dm² and a bath temperature of a) 35°C and b) 45°C.

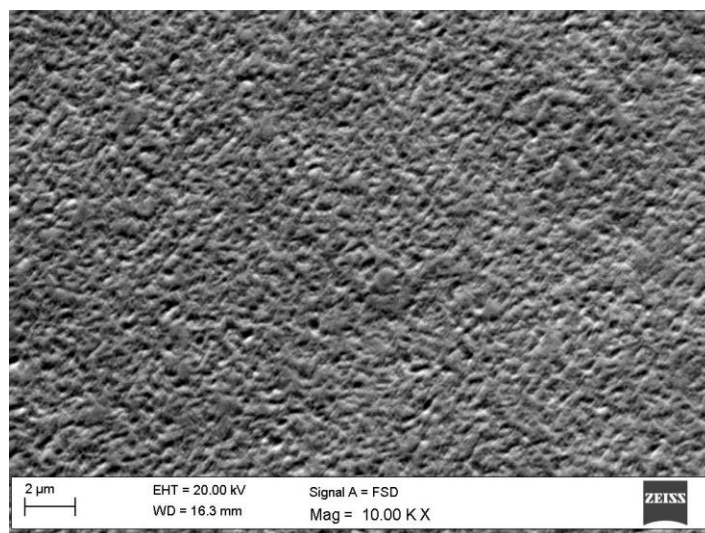


Figure 21: SEM image of sample produced with Electrolyte I at 20 A/dm² and a bath temperature of 55°C.

The samples produced with Electrolyte II in all plating conditions reveal very fine grains dispersed evenly in the microstructure. The representative microstructures of the samples are shown in figure 22.

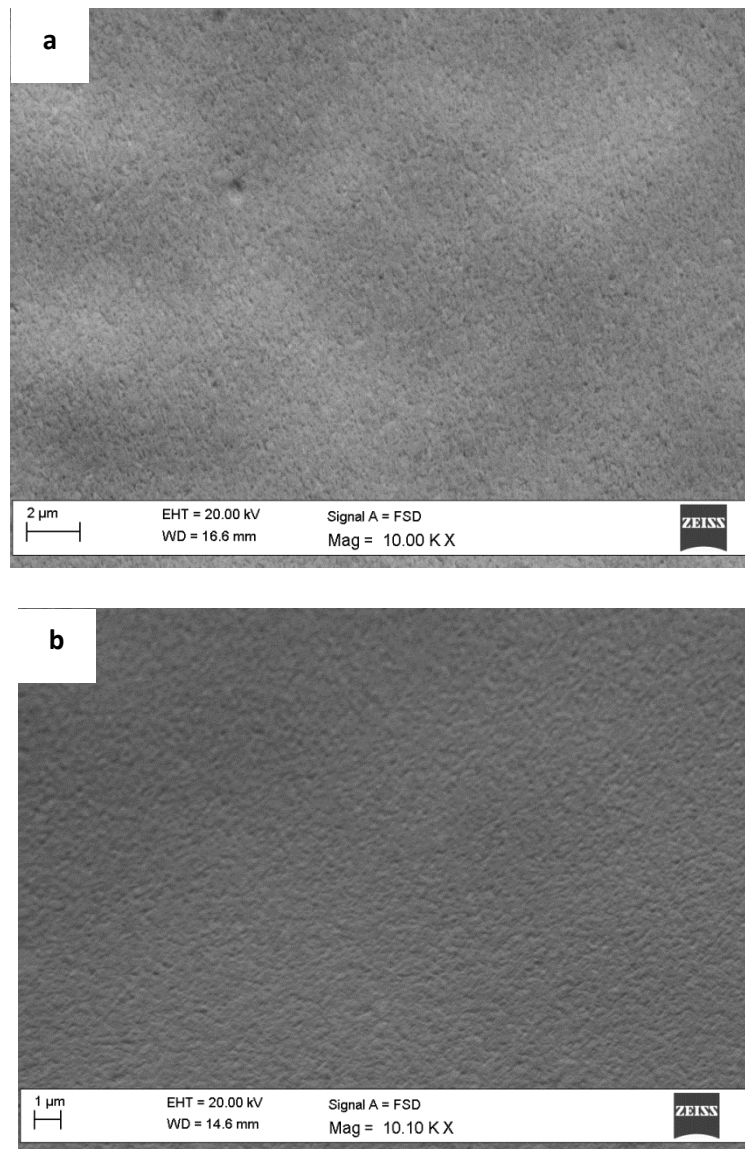


Figure 22: SEM images of samples produced with Electrolyte II at a) 10 A/dm² and 2.15M of Nickel Sulfamate concentration and b) 2 A/dm² and 2.44M of Nickel Sulfamate concentration.

3.3.3 EBSD Orientation Maps

The crystallographic orientation of the grains was obtained by the orientation map. The crystallographic direction of grains was colored with respect to the color key of inverse pole figure (figure 23). Noise reduction was applied in the measurement. So-called wild spikes were extrapolated to remove the single spots that are considered as the noise in the results. The extrapolation of zero solutions was performed with 6 neighboring pixels at a critical angle of 10°. During measurement of orientation maps, drift occurred which affected the precision of grain morphology analysis.

Only the orientation maps of the normal direction (Z-axis parallel to the growth direction) are shown. All samples produced with Electrolyte I show a very strong texture in $\langle 100 \rangle$ but a different grain morphology. The samples produced at 20 A/dm^2 with bath temperature of 35°C and 45°C , respectively, reveal coarse grain structure (figure 24). The microstructures of samples produced with Electrolyte I at high temperature with all current densities show a combination of fine and coarse grains distributed evenly in the investigated area (figure 25). However, a high fraction of zero solution (which most likely is due to the small grain size) can be observed in these samples (see Appendix).

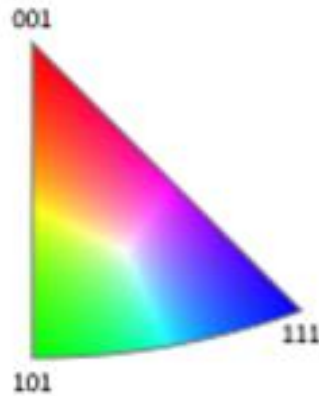


Figure 23: Color key for crystallographic orientations in inverse pole figure.

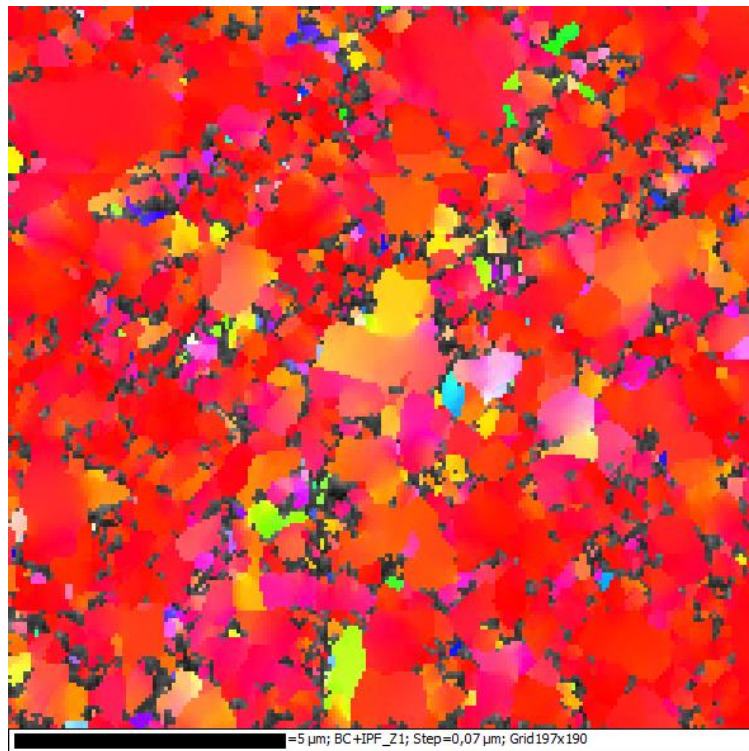
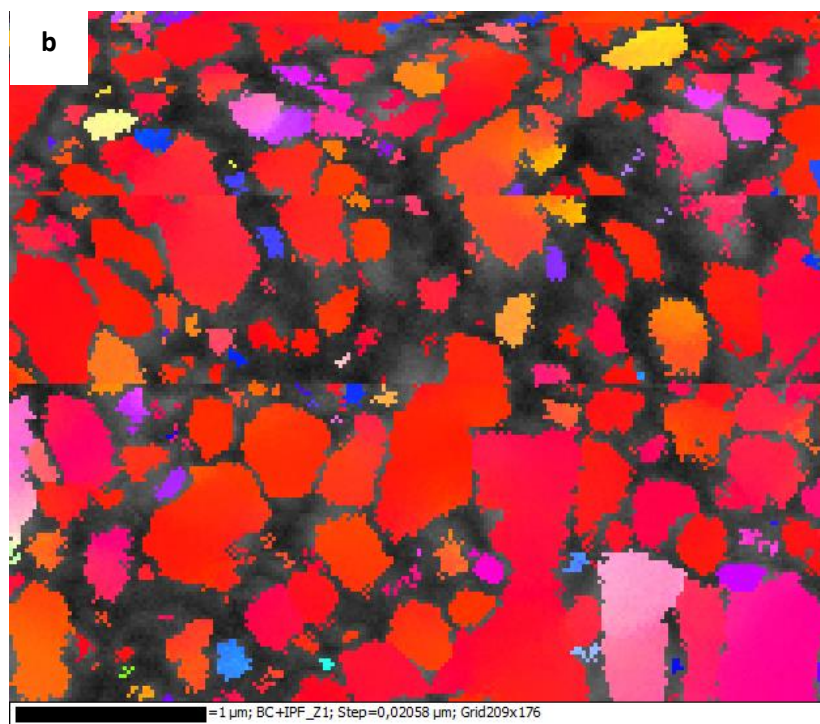
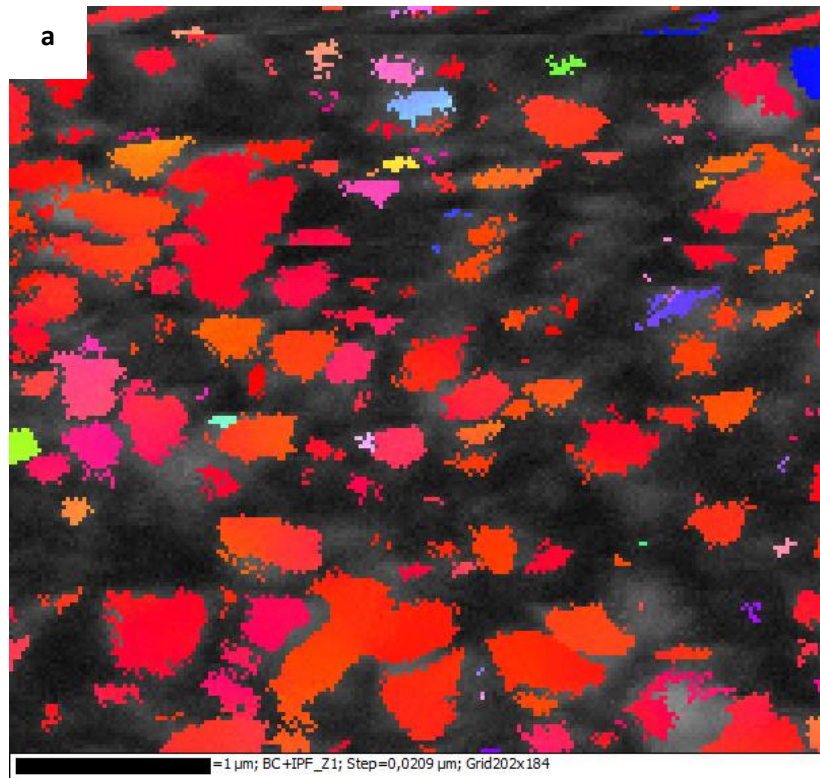


Figure 24: Orientation map of as-deposited Nickel film produced with Electrolyte I at 20 A/dm^2 and 45°C .



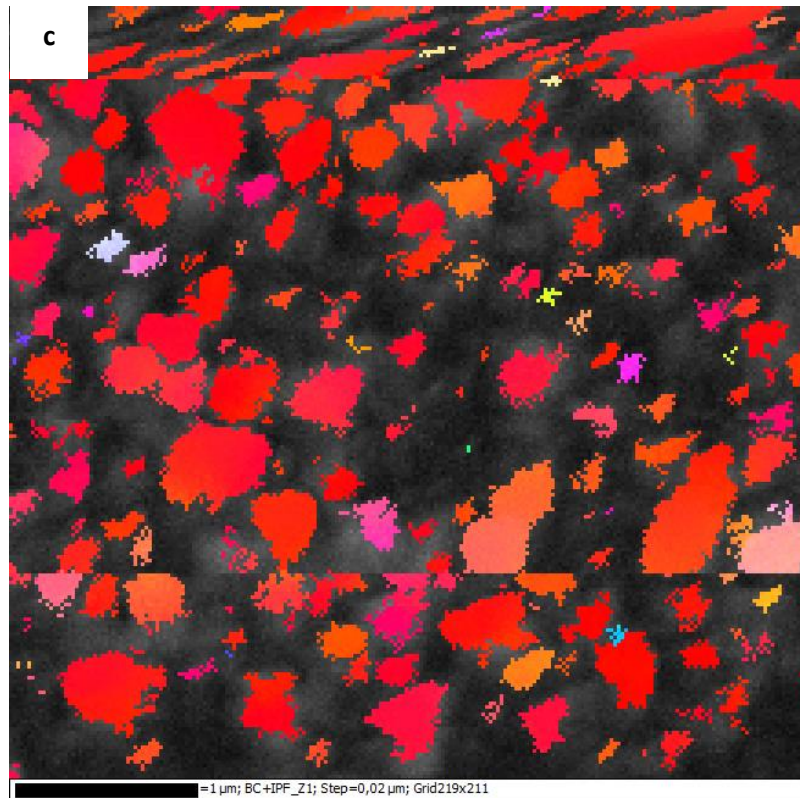
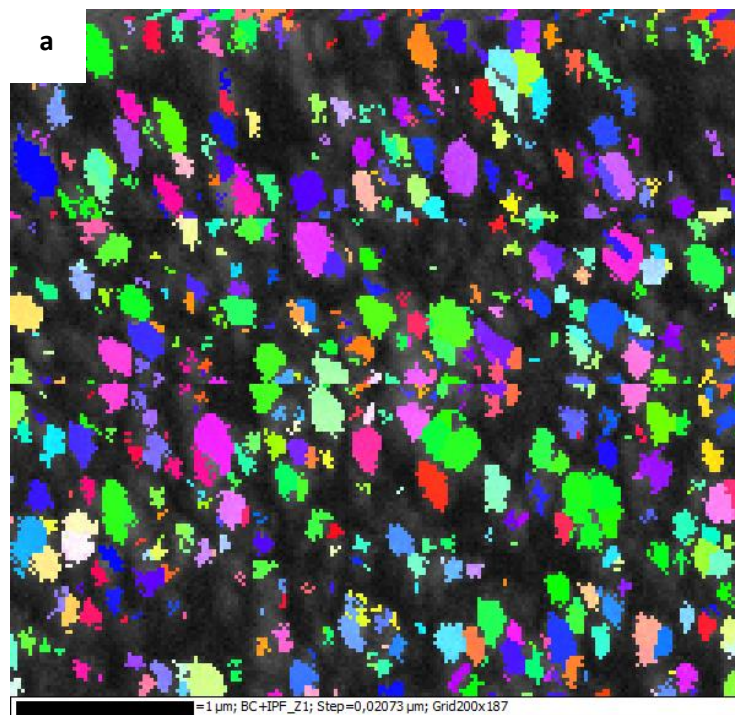
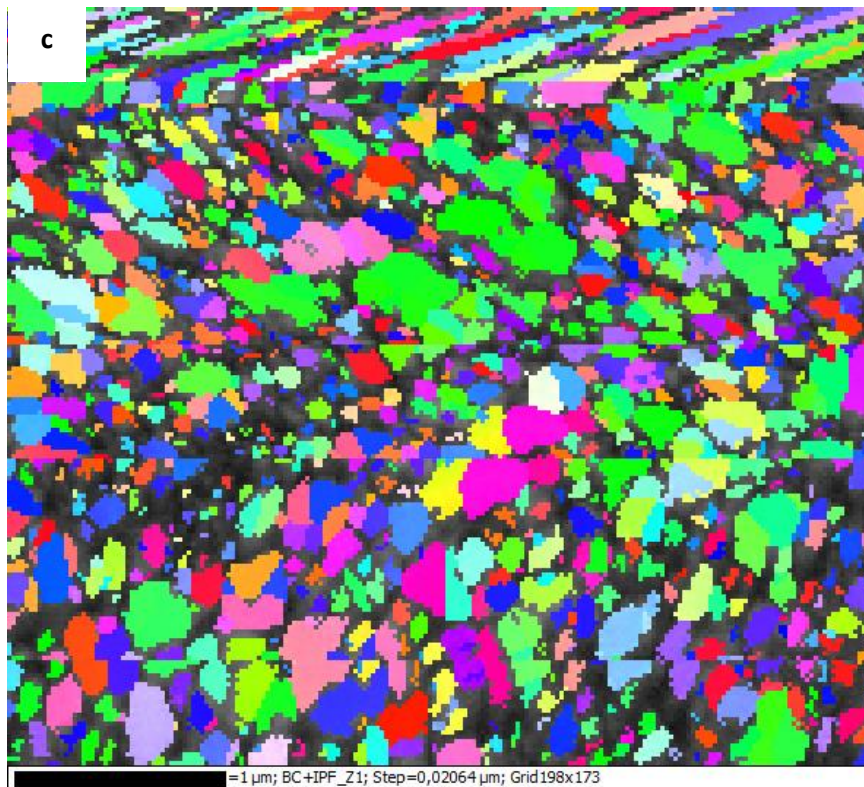
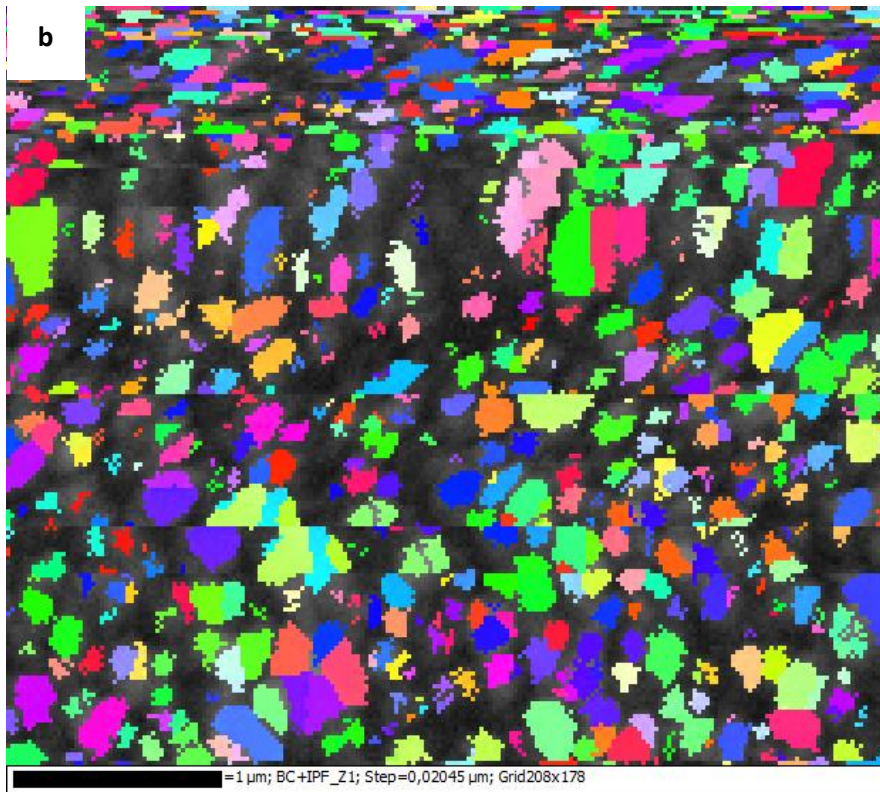


Figure 25: Orientation maps of as-deposited Nickel films produced with Electrolyte I at a) 2 A/dm² and 35°C, b) 10 A/dm² and 65°C and c) 20 A/dm² and 55°C.

The samples produced with Electrolyte II show very fine and well distributed grains with the variation in the grain colors. The representative maps of as-deposited Nickel films produced at different conditions are presented in figure 26.





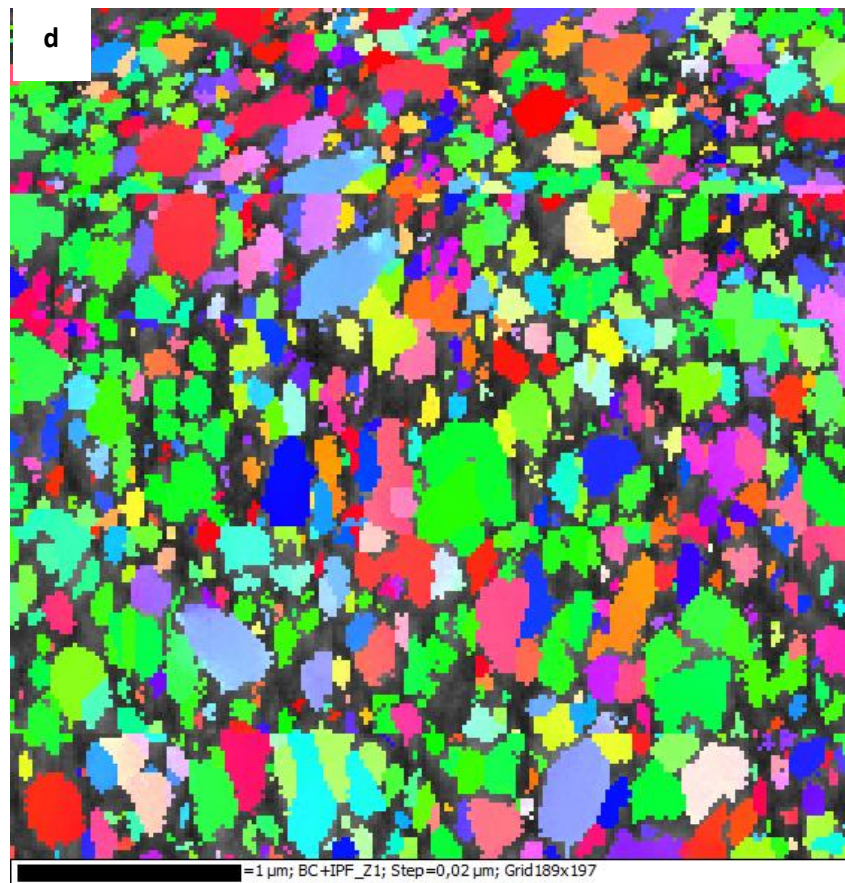


Figure 26: Orientation maps of as-deposited Nickel films produced with Electrolyte II at a) 2.15M and 2 A/dm², b) 2.44M and 2 A/dm², c) 2.89M and 2 A/dm², and d) 2.89M and 20 A/dm².

3.3.4 Grain Size Determination

Log-normal distribution histograms of the samples were plotted from the detected grains found in the orientation maps. The critical misorientation angle was set to 10°. In the present work, the consideration of grain boundary region and zero solution area were excluded. Also the drifting area which affect to the precision of the grain size calculation was excluded.

The analysis of the grain size of the samples produced with Electrolyte I at different bath temperatures and current densities is summarized as a bar chart in figure 27 (see Appendix for all data). The average grain sizes of the Nickel electrodeposits produced at 20 A/dm² at a bath temperature of 35°C and 45°C are 200±281 nm and 193±219 nm, respectively. The average grain size of 39±66 nm was the lowest average grain size found in the sample produced at 75°C. When prepared at temperature of 55°C and 65°C, Nickel electrodeposits reveal a slightly larger average grain size than the samples produced at 75°C.

In contrast to the sample produced at 20 A/dm², the samples produced at 2 A/dm² and 10 A/dm² show an average grain size lower than 100 nm at all plating temperatures.

As can be seen from the experimental data, bath temperatures in the range of 55°C to 75°C are providing Nickel electrodeposits to which the grain size is less influenced by

the current density. In contrast, at bath temperatures of 35°C and 45°C, the grain size of as-deposited Nickel films vary considerably with the current density.

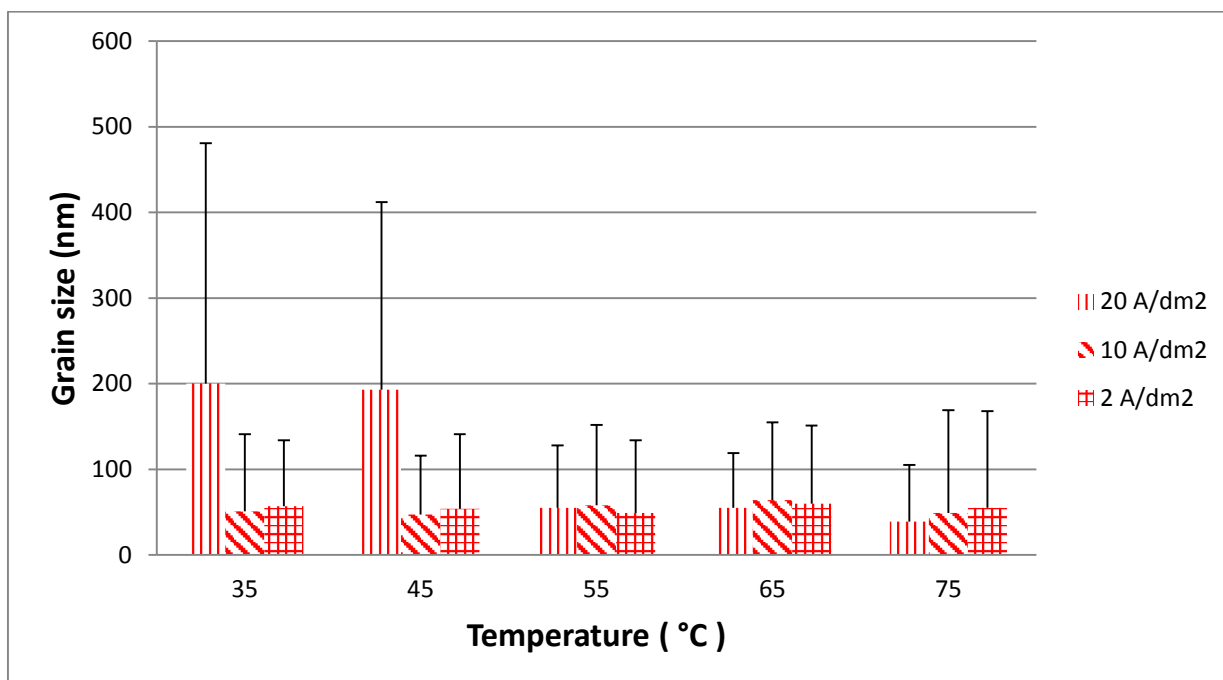


Figure 27: Diagram showing the average grain size for samples produced at different bath temperatures and current densities.

Nanostructure of Nickel electrodeposits can be observed in all samples produced with Electrolyte II. The average grain size of all investigated samples is displayed in table 10 and 11. From the tables, it can be seen that the current density and the amount of Nickel Sulfamate do not play an important role with respect to the grain size. However, with the increase the current density, an increase in grain size can be observed as shown in table 11, while the tendency of Nickel Sulfamate concentration effect on the average grain size has not been identified (table10).

Table 10: Grain size determination of samples produced with Electrolyte II at 20 A/dm² with different Nickel Sulfamate concentrations.

Nickel Sulfamate Concentration	Minimum Grain Size (nm)	Maximum Grain Size (nm)	Number of Investigated Grains	Standard Deviation (nm)	Average Grain Size (nm)
2.15 M	22.6	479	4464	62	56
2.44 M	22.7	630	5266	69	59
2.87 M	22.6	380	2388	45	49

Table 11: Grain size determination of samples produced with Electrolyte II at 2.44 M of Nickel Sulfamate concentration with different current densities.

Current Density	Minimum Grain Size (nm)	Maximum Grain Size (nm)	Number of Investigated Grains	Standard Deviation (nm)	Average Grain Size (nm)
2 A/dm²	23	316	1873	40	48
10 A/dm²	24	328	2088	41	49
20 A/dm²	23	630	5266	69	59

3.4 Pulse-Electroplating on Sandwich Material

Due to their outstanding mechanical properties with low weight, sandwich materials are starting to replace the conventional single-structure materials. To further improve their mechanical properties, pulse-electroplating was chosen to strengthen the sandwich material consisting of stainless steel plates to which Polyamide 6.6 fibers were attached. Since the Polyamide fibers are not conductive, Gold sputtering was used to provide a conductive coating on the fibers. As seen when using optical microscopy, the Gold particles were deposited homogeneously on the fiber surface and covered the entire length of the fibers down to the adhesive layer (figure 28a). After two-hour pulse-electroplating, a Nickel electrodeposit could clearly be seen on the fibers situated on the sample edges and in the area around the Copper wires which were attached to improve the conductivity between the fibers and the substrate. Fibers in the middle of the sample and further away from the Copper wires were not covered to the same extent (figure 28b and 28c) even though a Gold layer was present on the fiber surface.

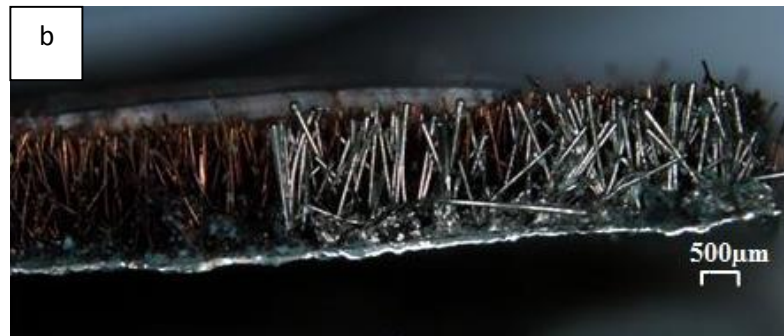
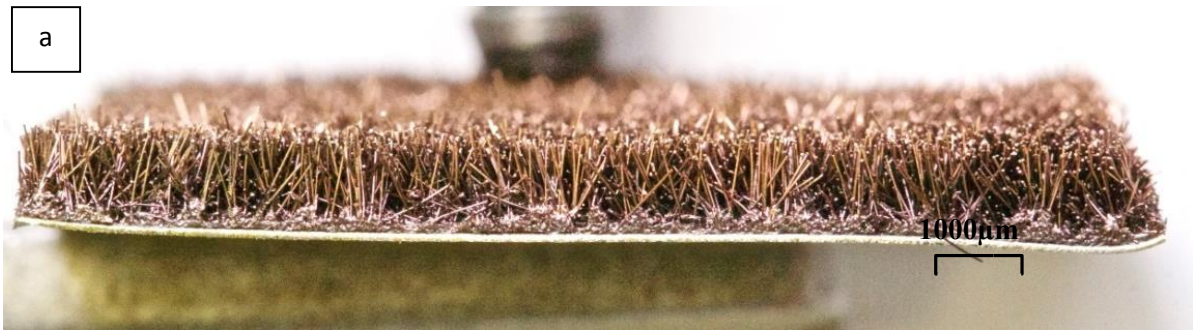


Figure 28: Electrodeposition of Nickel on polymer fibers a) Cross section image showing fibers after Gold sputtering, b) Cross section image showing the electrodeposited Nickel coating on fibers, and c) Image showing the electrodeposited Nickel coating on fibers at the sample edge and close to the attached copper wires.

4 Discussion

4.1 Effect of Current Density and Temperature

The results obtained in the present work show that grain size is influenced by the current density and plating temperature. The grain size increases with the increase in current density. At each plating temperature from 35°C to 65°C, the grain refinement can be observed when the current density decreases. This behavior is consistent with Cziráki et al. [27] where they suggest that the grain size increasing with the increase in current density. This is due to the depletion of Nickel ions on the interface between the deposit layer and electrolyte. The low concentration of the Nickel ions on the cathode surface leads to the low nucleation rate and results in a coarse-grain structure [14]. While, the deposition rate of as-deposited Nickel films on the substrate is still increased with the increase in current density [18]. However, there are some studies [21][28] that reported the effect of current density on a grain refinement differently in the way that the grain size decreases with the increase in current density. This is attributed to the increase of nucleation rate in electrodeposit when the current density increases and as a result, a fine-grain structure is obtained.

The temperature of the plating bath has two opposite effects on the electrodeposition process. Firstly, the thermodynamic driving force decreases with increasing the bath temperature and results in the increase of critical size of the nuclei. This leads to a low nucleation rate. Secondly, a higher bath temperature enhances the kinetic driving force of the process and results in a higher nucleation rate. In electroplating, the deposition of material is controlled only by the kinetic mechanism since the thermodynamic mechanism can be neglected. The nucleation rate then increases and a fine-grain microstructure can be obtained when the bath temperature is increased [21]. This behavior can be observed in the results of the present work where the grain size of as-deposited Nickel reduces reasonably from 200 nm to 50 nm with increasing the temperature from 35°C to 75°C when using a current density of 20A/dm² as plating parameter.

The as-deposited Nickel in the present work shows a strong preferred <100>- orientation in the growth direction. This is also reported by Rasmussen et al. [29] where the texture of <100> can be found in a wide range of current densities. Furthermore, when comparing the results of the present work with the texture diagram proposed by Amblard et al. [10], <100> is the dominant texture at a current density above 2 A/dm² and at a pH value of 4 which is the same pH value used for the electrolyte in this project.

4.2 Effect of Nickel Sulfamate Concentration and Current Density

The grain refinement can be observed with lowering the current density in Nickel electrodeposition. According to literature [27], the high deposition rate causes the depletion of Nickel ions at the deposits-electrolyte interface at high current density which leads to a coarse-grain structure. As can be seen in this experiment, the average grain size of as-deposited Nickel films decreases from 59±69 nm to 48±40 nm when the current density decreases from 20 A/dm² to 2 A/dm².

The samples produced with Electrolyte II show a weak <110>-texture. This indicates that the samples are formed in the growth mode inhibited by H_{ads} [10][11][12]. This is in

accordance with the results from Klement et al. [30] where the samples produced in an additive -free bath contain a weak $\langle 110 \rangle$ -texture parallel to the growth direction. The same additive-free bath is used in this thesis work.

4.3 Pulse-Electroplating on Sandwich Material

After the electroplating process, the electrodeposited coating layer on the fibers was investigated. Fibers situated at the edge of the sample and also a small region around the Copper wires was covered by a Nickel electrodeposit. This result could be related to the conductivity of material. The surface that was easily exposed to the Au-ions could become more conductive than the region located in the center of the sample. In addition, even if the fibers were Gold-sputtered but they were not connected to each other and to the substrate, the pulse-electroplating process could not be achieved.

5 Conclusion

In this thesis work, the effect of current density, temperature and Nickel Sulfamate concentration on the formed microstructure of Nickel electrodeposit was investigated. The results show that the microstructures of as-deposited Nickel films are strongly influenced by the current density and temperature. A grain refinement can be observed with the increase in bath temperature and the decrease in current density. This is due to the fact that the high migration rate of Nickel ions in high temperature range and the sufficient amount of Nickel ions on the cathode surface in low current density enhances the nucleation rate of Nickel electrodeposits. Nickel electrodeposits produced with Electrolyte I exhibit the $\langle 100 \rangle$ -texture which is the usual texture presented in the pH value of 4 for the wide range of current densities. In contrast, the samples produced with Electrolyte II reveal a weak $\langle 110 \rangle$ -texture which is the inhibited growth mode influenced by H_{ads} . The further investigation is required for the identification of Nickel Sulfamate concentration effect on the formed microstructure since a low number of samples was investigated in this present work.

The pulse-electroplating technique can be applied to strengthen the HybrixTM sandwich material. However, the process is dependent on the electrical conductivity between fibers and substrate.

Future Recommendations

1. In this project, the effect of the current density, temperature and Nickel Sulfamate concentration have been investigated. Considering the wide number of the process parameters that could affect the formed microstructure, the effect of parameters such as pH value, duty cycle, distance between anode and cathode would be of interest for further investigations. In addition, saccharin which acts as a grain refiner could be added in the electrodeposition process and its effect could be further investigated.
2. With regard to Hybrix™ sandwich material, another set of pulse-electroplating operations could be performed for another material where the present non-conductive epoxy adhesive is replaced by a conductive adhesive. The replacement will increase the conductivity between fibers and substrate and the pulse-electroplating could provide better results.

Reference

- [1] M. Paunovic and M.Schlesinger, *Modern electroplating*, 5th ed. New Jersey: John Wiley & Sons, Inc., 2011.
- [2] U. Erb, K.T. Aust, G. Palumbo, “Electrodeposited nanocrystalline metals, alloys and composites,” in *Nanostructured materials – processing, properties, and applications*, C.C. Koch, Ed., 2nd ed. New York: William Andrew, 2007, pp. 235-292.
- [3] R. Abdel-Karim and A. F. Waheed, “Nanocoatings,” in *Modern Surface Engineering Treatments*, A. Mahmood, Ed.:Intech, 2013.
- [4] U. Erb and A.M. El-Sherik, “Nanocrystalline metals and process of producing the same,” U.S. Patent 5 352 266, Oct 4, 1994.
- [5] U. Erb, A.M. El-Sherik, G. Palumbo and K.T. Aust, “Synthesis, structure and properties of electroplated nanocrystalline materials,” *Nanostructured Mater.*, Vol. 2, no. 2, pp. 383–390, 1993.
- [6] U. Erb and A.M. El-Sherik, “Synthesis of bulk nanocrystalline nickel by pulsed electrodeposition,” *J. Mater. Sci.*, Vol. 30, pp. 5743–5749, 1995.
- [7] H. Gleiter, “Nanocrystalline Materials,” *Prog. Mater. Sci.*, Vol. 33, pp. 223–315, 1990.
- [8] U. Erb, “Electrodeposited nanocrystals: synthesis, properties and industrial applications,” *Nanostruct. Mater.*, Vol. 6, pp. 533–538, 1995.
- [9] N.A. Pangarov, “Preferred orientations in electrodeposited metals,” *J. Electroanal. Chem.*, Vol. 9, pp. 70-85, 1965.
- [10] J. Amblard and M. Froment, “New interpretation of texture formation in nickel electrodeposits,” *Faraday Symp. Chem. Soc.*, Vol. 12, pp. 136-144, 1977.
- [11] J. Amblard, I. Epelboin, M. Froment, and G. Maurin, “Inhibition and nickel electrocrystallization,” *J. Appl. Electrochem.*, Vol. 9, no. 4, pp. 233–242, 1979.
- [12] C. Kollia, N. Spyrellis, J. Amblard, M. Froment, and G. Maurin, “Nickel plating by pulse electrolysis: textural and microstructural modifications due to adsorption/desorption phenomena,” *J. Appl. Electrochem.*, Vol. 20, pp. 1025–1032, 1990.
- [13] A. Shibata, H. Noda, M. Sone, and Y. Higo, “Microstructural development of an electrodeposited Ni layer,” *Thin Solid Films*, Vol. 518, no. 18, pp. 5153–5158, 2010.
- [14] I. Bakonyi, E. Tóth-Kádár, L. Pogány, Á. Cziráki, I. Geröcs, K. Varga-Josepovits, B. Arnold, and K. Wetzig, “Preparation and characterization of d.c.-plated

- nanocrystalline nickel electrodeposits,” *Surf. Coatings Technol.*, Vol. 78, no. 1–3, pp. 124–136, 1996.
- [15] I. Bakonyi, E. Tóth-Kádár, T. Tarnóczy, L. K. Varga, Á. Cziráki, I. Geröcs, and B. Fogarassy, “Structure and properties of fine-grained electrodeposited nickel,” *Nanostructured Mater.*, Vol. 3, no. 1–6, pp. 155–161, 1993.
- [16] Y. Xuetao, W. Yu, S. Dongbai, and Y. Hongying, “Influence of pulse parameters on the microstructure and microhardness of nickel electrodeposits,” *Surf. Coatings Technol.*, Vol. 202, no. 9, pp. 1895–1903, 2008.
- [17] R. T. C. Choo, J. M. Toguri, a. M. El-Sherik, and U. Erb, “Mass transfer and electrocrystallization analyses of nanocrystalline nickel production by pulse plating,” *J. Appl. Electrochem.*, Vol. 25, no. 4, pp. 384–403, 1995.
- [18] F. Ebrahimi and Z. Ahmed, “The effect of current density on properties of electrodeposited nanocrystalline nickel,” pp. 733–739, 2003.
- [19] A. M. El-Sherik, U. Erb, and J. Page, “Microstructural evolution in pulse plated nickel electrodeposits,” *Surf. Coatings Technol.*, Vol. 88, pp. 70–78, 1997.
- [20] S. Ravi, K. V. Ganesh, A. Ramanathan, J. Annamalai, and P. K. Jaiswal, “Development of Nanocrystalline Nickel Coating for Engineering Applications,” *Key Eng. Mater.*, Vol. 443, pp. 487–492, 2010.
- [21] A. M. Rashidi and A. Amadeh, “Effect of electroplating parameters on microstructure of nanocrystalline nickel coatings,” *J. Mater. Sci. Technol.*, Vol. 26, no. 1, pp. 82–86, 2010.
- [22] M. Paunovic and M. Schlesinger, *Fundamentals of Electrochemical Deposition*, 2nd ed. New Jersey: John Wiley & Sons, Inc., 2006.
- [23] J.W. Dini, *Electrodeposition - The Materials Science of Coatings and Substrates*. New Jersey: Noyes Publications, 1993
- [24] H. Natter and R. Hempelmann, “Tailor-made nanomaterials designed by electrochemical methods,” *Electrochim. Acta*, Vol. 49, no. 1, pp. 51–61, 2003.
- [25] O. Engler, V. Randle, *Introduction to Texture Analysis: Macrotecture, Microtexture and Orientation Mapping*, 2nd ed. Boca Ratan: CRC Press, 2010.
- [26] Oxford Instrument Plc, “EBSD Electron Backscatter Diffraction Analysis,” [Online]. Available: <http://www.ebsd.com> [Accessed: May. 4, 2015].
- [27] Á. Cziráki, B.F. Fogarassy, I. Geröcs, E. Tóth-Kádár, I. Bakonyi, *J. Mater. Sci.*, Vol. 29, pp. 4771, 1994.
- [28] P.Q. Dai, Hui Yu and Q. Li: *Trans. Mater. Heat Treatment*, Vol. 25, pp. 1283, 2004. (in Chinese)

- [29] A.A. Rasmussen, P. Møller, M.A.J. Somers, "Microstructure and thermal stability of nickel layers electrodeposited from an additive-free sulphamate based electrolyte," *Surface and coating technology*, Vol. 200, pp. 6037-6046, 2006.
- [30] U. Klement, C. Oikonomou, R. Chulist, B. Beausir, L. Hollang, W. Skrotzki, "Influence of Additives on Texture Development of Submicro- and Nanocrystalline Nickel," *Materials Science Forum*, Vols. 702-703, pp 928-931, 2012.

Appendix: Grain Size Determination

In the following tables, the results from grain size determination of as-deposited Nickel films produced with Electrolyte I and II are summarized. All the samples were investigated by EBSD with the scanning step size of 0.02 μm , except the samples produced at 2 A/dm^2 with a bath temperature of 35°C and 45°C which were investigated with the scanning step size of 0.07 μm .

Table 12: Summary of the results from the grain size determination of as-deposited Nickel films produced with Electrolyte I by varying current density and temperature.

Current Density (A/dm ²)	Temperature (°C)	pH Value	Number of Investigated Grains	Zero solution Phase Fraction (%)	Standard Deviation (nm)	Average Grain Size (nm)
2	35	3	528	70.96	77	57
	45	3	505	63.58	87	54
	55	4	462	57.35	85	49
	65	4	812	50.40	91	60
	75	4	417	51.11	113	55
10	35	4	502	65.89	90	51
	45	4	436	80.71	69	47
	55	4	483	60.37	94	58
	65	3	582	43.43	91	64
	75	4	371	47.87	120	49
20	35	2-3	1473	23.16	281	200
	45	2-3	1761	20.46	219	193
	55	2-3	739	69.42	73	55
	65	2-3	744	49.77	64	55
	75	3	483	76.61	66	39

Table 13: Summary of the results from the grain size determination of as-deposited Nickel films produced with Electrolyte II by varying Nickel Sulfamate concentration and current density.

Nickel Sulfamate Concentration (M)	Current Density (A/dm ²)	pH Value	Number of Investigated Grains	Zero Solution phase Fraction (%)	Standard Deviation (nm)	Average Grain Size (nm)
2.15	2	4	1341	70.25	43	48
	20	4	4464	66.27	62	56
2.44	2	4-5	1873	60.37	40	48
	10	4	2088	51.16	41	49
	20	4	5266	60.04	69	59
2.87	2	4	2693		39	47
	20	4	2388	40.21	45	49

